Photonuclear Sum Rules for ^{6}He

by

Raymond Goerke

A THESIS SUBMITTED IN PARTIAL FULFILLMENT
OF THE REQUIREMENTS FOR THE DEGREE

Bachelor of Science

in

THE FACULTY OF SCIENCE
(Combined Honours Physics and Mathematics)

The University Of British Columbia
(Vancouver)

April 2011

Abstract

We perform the *ab-initio* calculation of photonuclear sum rules for ^{4}He and ^{6}He using semi-realistic potentials. Our results include the first *ab-initio* calculation of the electric polarizabililty of ^{6}He. We perform the calculation by expanding the the wavefunctions in a Hyperspherical Harmonic basis and solving the Schrödinger equation exactly. Model space trunction effects are estimated by incrementing the size of the Hilbert space, and evaluating the convergence pattern. We also compute sum rules by integrating the theoretically computed cross section available from the literature. Full convergence is not yet achieved. A discussion of the preliminary results is presented. Future work, taking advantage of negligible symmetries in the hyperspherical harmonic basis, should be able to achieve full convergence.

Table of Contents

Abstract . . . . . **ii**

Table of Contents . . . . . **iii**

List of Tables . . . . . **iv**

List of Figures . . . . . **v**

Acknowledgements . . . . . **vi**

1 Introduction **1**

2 Theoretical Framework **5**

2.1 Electric Polarizability 5

2.2 Photoabsorption Cross Sections 6

2.2.1 Photonuclear Moments and Sum Rules 8

2.3 Sum Rules and Nuclear Observables 8

2.3.1 Polarizability Sum Rule 9

2.3.2 Thomas-Reiche-Kuhn Sum Rule 9

2.3.3 Bremstrahlungs Sum Rule 10

3 Computational Techniques **12**

3.1 Hyperspherical Basis 12

3.2 Evaluation of Matrix elements 13

3.3 The Lanczos Algorithm 15

3.4 Implementation 17

3.4.1 Calculating the Sum Rules 18

4 Calculating the Full Continuum Response 21

5 Results 24
5.1 Testing the Sum Rule Code 24
5.2 Parallelization 26
5.3 Sum Rules 28
5.4 Photoabsorption Cross Section 32
5.5 Conclusions 34

Bibliography 35

A Complete Derivations of Sum Rule Formulas 38
A.1 Thomas-Reiche-Kuhn Sum Rule 39
A.1.1 39
A.1.2 39
A.2 Bremstrahlung Sum Rule 45
A.2.1 45
A.2.2 45
A.2.3 46
A.2.4 47
A.2.5 47
A.2.6 48
A.3 Polarizability Sum Rule 50
A.3.1 50

B Hyperspherical Formalism 51
B.1 Jacobi Coordinates 51
B.2 Hyperspherical Coordinates and the Laplace Operator 52
B.3 Hyperspherical Harmonics 55
B.4 Hyperspherical Basis 57

List of Tables

Table 1.1 *Ab inito* calculations of electric dipole polarizability of various nuclei. Note there is no value at all for ^{6}He. 3

Table 5.1 Previous calculations from Gazit et al. [1] of the sum rules using the Lanzcos coefficients are compared with our calculations using the same Lanzcos coefficients to test the validity of the sum rule code. We compared our results for largest model spaces denoted by $K_{\max}$. 24

Table 5.2 Convergence error in the polarizability sum rule for ^{4}He with the simple potential models. The value is estimated as the percentage change from the $K_{\max} = 10$ to $K_{\max} = 12$ model space size. 26

Table 5.3 Theoretical and experimental results for the polarizability of ^{4}He. The two other theoretical values were computed using more realistic two-body potential models and included three-body forces. The experimental values were obtained through Compton scattering. 26

Table 5.4 Convergence error estimate for sum rules. Computed as the percentage change in the value from the second-largest to the largest model space. 30

Table 5.5 Estimated model-dependent error. Computed as the standard deviation from the mean value among potential models used. . 32

Table 5.6 Binding energies and root mean square radii for ^{6}He and ^{4}He using $K_{\max} = 12$. The error in the last digit is taken to be the difference between the $K_{\max} = 12$ and $K_{\max} = 10$ values. 32

Table 5.7 PSR of ^{6}He calculated by integrating the cross section compared to sum rule approach. 34

List of Figures

Figure 1.1 A nuclear chart showing the relative sizes of light. Highlighted are ^{4}He, ^{6}He, and some other halo nuclei. 3

Figure 5.1 Polarizability of ^{4}He computed using different sized model spaces denoted by maximum grandangular momentum $K_{\max}$. The experimental points were obtained by Compton scattering with experimental error indicated by the shaded regions. . . . 25

Figure 5.2 A cartoon of how the matrix elements in a hermitian matrix can be allocated efficiently between four processors. The colour of each matrix element corresponds to the processor it is assigned to. 27

Figure 5.3 TRK sum rule computations for different sizes of model space characterized by max grandangular momentum $K_{\max}$. 29

Figure 5.4 BSR sum rule computations for different size of model space characterized by max grandangular momentum $K_{\max}$. 30

Figure 5.5 Polarizability sum rule computations for different sizes of model space characterized by max grandangular momentum $K_{\max}$. The experimental point is from Pachucki and Moro [2] using Coulomb breakup, the shaded region is the experimental error. 31

Figure 5.6 The photoabsorption cross section computed by Bacca et al. [3] using the AV4' potential. The inverse-square energy-weighted cross section is included (scaled to be visible) to show how the lack of data going to infinity does not effect the value of the PSR. The model space size used to compute the cross section was $K_{\max} = 12$. 33

Figure B.1 The (unnormalized) Jacobi coordinates for four particles. The $\tilde{\eta}_i$ vectors point along the direction of the normalized η_i given by equation (B.1). 52
Figure B.2 Geometric interpretation of the recursive generation of hyperspherical coordinates 53

Acknowledgements

I would like to thank TRIUMF for their summer student program where I learnt much of the background and theory involved in this project. I'm grateful to the UBC Faculty of Science, Department of Physics and Astronomy, and Undergraduate Physics Society for funding me to present some of this work at the Canadian Undergraduate Physics Conference. I would like to thank my parents, without whose love and support I could not have gotten this far. Finally, I owe an especially heartfelt thank you to Sonia Bacca, my supervisor, who has taught me and helped me enormously over the last year.

Chapter 1

Introduction

The interaction of nucleons with the electromagnetic field (photons or electrons) is well understood and enables a clear separation of the analysis of the probe from that of the nuclear dynamics, which is still not well understood. In particular, *ab-initio* methods are very valuable for understanding nuclear dynamics. An *ab-initio* calculation is "from first principles" in that it describes the quantum mechanical problem as nucleons interacting via a nuclear Hamiltonian. In cases where the Schrödinger equation is solved without introducing approximations, we say such calculations are exact. In this work we perform exact, *ab-initio* calculations and the terms are used interchangeably[1].

Exact calculations also allow us to test the role that three-body forces play in the determination of electromagnetic observables. Understanding what observables are sensitive to many-body forces is important for constraining self-consistent models of many-body forces such as Chiral Perturbation Theory [4].

Due to the obvious computational constraints, exact calculations have been restricted to the light nuclei with mass numbers about $A \leq 12 - 16$ for bound states. In the case of the electromagnetic breakup observables, which depend on continuum properties of the nucleus, i.e. properties of unbound states, then typically we are restricted to about $A \leq 7$. Often, the full continuum response must be calculated in these situations, for which some powerful tools including the Lorentz Integral Transform technique have been developed.

[1] Note that in the literature this may not generally be the case.

In this work, I have studied the photonuclear sum rules of light nuclei including ^{4}He and ^{6}He. Photonuclear sum rules are related to the moments of the photonuclear cross section which can be compared with experiment. I have used semi-realistic potentials in my calculations, i.e. potentials that do not include high l parts of the interaction, to simplify the calculations. This may lay the groundwork for more sophisticated future calculations.

Of particular interest is the polarizability sum rule, which allows a direct calculation of the electric polarizability of the nucleus. When a nucleus is placed in an electric field, the field displaces the nucleons and creates a dipole moment in the nucleus centre of mass. In the weak field limit, the induced dipole is directly proportional to the external field:

$$D_z = \alpha_E E_z. \tag{1.1}$$

Where α_E is the polarizability of the nucleus. Of the several nuclear systems we can study, "halo" nuclei like ^{6}He are of particular interest. The name "halo" is given to nuclei with anomalously large matter radius attributed to loosely bound outer neutrons. Scattering experiments suggest that these nuclei have radii much larger than other isotopes of the same element and are often comparable to nuclei with much larger mass numbers. For example, while the radius of ^{4}He is measured to be about 1.7 fm [5], the radius of ^{6}He is found to be about 3.7 fm [6]. Figure 1.1 plot the relative size of light nuclei. For ^{6}He, the neutron halo makes the electric polarizability markedly interesting because we would expect it to be much larger than other helium isotopes, especially the extremely compact ^{4}He. The diffuse neutron halo also makes it particularly difficult to achieve convergent results with ^{6}He as many basis states are needed to capture the long tail.

In Table 1.1, I have presented previous *ab-initio* calculations of nuclear polarizability of hydrogen and helium isotopes. Note the lack of values for ^{6}He. I will be presenting the first computations of this observable for ^{6}He. There is a single experimental measurement of the polarizability of ^{6}He, and the estimated error on this value is large due to the method used to extract it from the data [7].

The electric polarizability also has importance in high-precision atomic spectroscopy. Here, accurate measurements of the energy difference between atomic

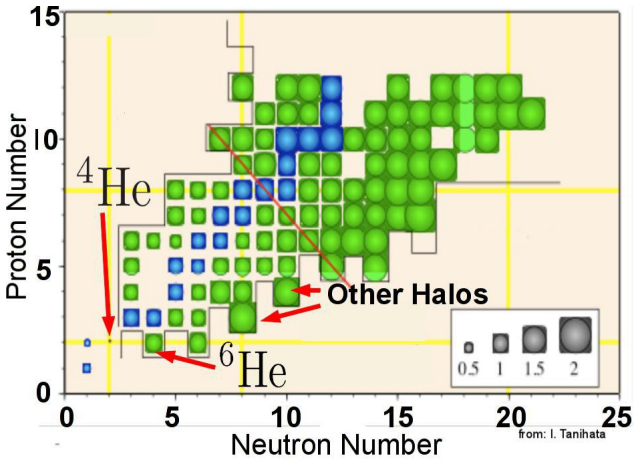

Figure 1.1: A nuclear chart showing the relative sizes of light. Highlighted are ^{4}He, ^{6}He, and some other halo nuclei.

Nucleus	α_E(fm^3)	Reference
^{2}H	0.6328(17)	[8]
	0.6314(19)	[9]
^{3}H	0.139(2)	[10]
	0.139	[11]
^{3}He	0.149(5)	[10]
	0.145	[12]
^{4}He	0.0683(8)(14)	[10]
	0.0655(4)	[1]
^{6}He		

Table 1.1: *Ab inito* calculations of electric dipole polarizability of various nuclei. Note there is no value at all for ^{6}He.

energy levels (also called the transition frequency when referring to the resonant laser frequency) are becoming precise enough to see effects of nuclear structure [13]. In general, transition frequencies between S states in single-electron atoms and ions are determined by a initial value derived from a relativistic hydrogen-atom model, to which corrections are applied resulting from Quantum Electrodynamics (QED) and nuclear effects. The QED effects are much more important than nuclear effects in light nuclei, but recent progress in this area ensures the highest-order terms have already been calculated and remaining terms are estimated to have smaller effect than nuclear corrections [14]. The biggest nuclear corrections are associated with the non-zero charge radius of the nucleus, and due to the fact that it is not a rigid body. The latter effect is dominated by the electric polarizability, which is effectively a measure of how much the electron deforms the nucleus and "drags" the deformation as it orbits (in analogy to the way the moon creates the tides).

Recent measurements of hydrogen-like atoms and ions can be used as measurements of the charge radius by fitting the charge-radius correction to the experimental data while using calculated values for the QED and polarization corrections [10], and it has been shown that these kinds of measurements agree with the results from direct measurements of proton radius using electron scattering [15, 16].

Although at the current stage [17], electric polarizability plays only a marginal role in comparison to other contributions to atomic observables in the case of six-body nuclei, future improvements of experimental precision will require reliable values for this observable.

While the electric polarizability is perhaps the most interesting observable in terms of its implications to other research, the other sum rules I have studied include the bremsstrahlungs sum rule (BSR) and the Thomas-Reiche-Kuhn (TRK) sum rule, which have mostly theoretical interest. The former is relatable in several ways to the geometric structure of the nucleus. This may be useful in understanding the neutron halo in ^{6}He and potentially other halo nuclei. The later is related to the so-called TRK enhancement factor, which is used in the study of nuclear potential models by providing a way to quantify the role of exchange effects in the interaction (for more details, see A.1).

Chapter 2

Theoretical Framework

In this chapter we discuss the photonuclear cross section as a way to gain information about nuclear observables coupled to the electromagnetic field, and the use of sum rules to relate photonuclear moments to tractable computable expressions. Before introducing the more generic case, we consider a concrete example with a classical analogue; namely, the electric polarizability of a nucleus, which can be thought of as the effect of a perturbation by a small external electric field.

2.1 Electric Polarizability

The perturbed Hamiltonian resulting from applying an electric field with magnitude E_{ext} pointed along the z direction is $H = H_0 - E_{\text{ext}} D_z$, where D_z is the z component of the induced dipole moment. Due to parity symmetry of the ground state, the first order correction $\langle 0|$ (-E_{ext} D_z)$|0\rangle$ is zero. The second order correction is

$$E_0^2 = -\frac{1}{2}\alpha E_{\text{ext}}^2,$$

where α corresponds to the classical definition of polarizability; namely, if $|0\rangle$ is the ground state of the full Hamiltonian H we have:

$$\alpha_E = \lim_{E_{\text{ext}} \to 0} \frac{\langle 0| D_z |0\rangle}{E_{\text{ext}}}.$$

By using the standard perturbation theory arguments, we can thus show

$$\alpha_E = \alpha \frac{\sum_n |\langle n| D_z |0\rangle|^2}{E_n - E_0}. \tag{2.1}$$

Where the sum ranges over all possible final states $|n\rangle$, including continuum states. By convention, the fine structure constant α is included, which absorbs various electromagnetic units from the dipole operator. In this work, α_E will always refer to the electric polarizability while α will always refer to the fine structure constant.

In the following sections we will show that equation (2.1) can be calculated as a sum rule for the photonuclear cross section and that, in a similar way, other sum rules, including the bremmstrahlungs and Thomas-Reiche-Kuhn sum rule, will lead to analagous formulas related to other electromagnetic observables with theoretical interest.

2.2 Photoabsorption Cross Sections

The photoabsorption cross section can be defined in terms of a response function $R(\omega)$, where ω is the photon energy:

$$\sigma^\gamma(\omega) = \mathscr{G}\omega R(\omega),$$

where $\mathscr{G}$ is a constant which we define as $\mathscr{G} = 4\pi^2\alpha$.

The response function encodes the effect of a small perturbation by a photon to the system. For the most general effect of photoabsorption, the response function is written in terms of the electromagnetic current four-vector $J^\mu = (\rho, \mathbf{j})$.

$$R(\omega) = \sum_n |\langle n| J^\mu(\mathbf{q}) |0\rangle|^2 \delta(E_n - (E_0 + \omega)), \tag{2.2}$$

where $\mathbf{q}$ is the momentum transfer (for photoabsorption $\mathbf{q} = \omega$). As before, the sum over final states must also include an integral over continuum states.

We perform a multipole decomposition on J^μ, first by expanding ρ in terms of

Coulomb multipoles:

$$\rho(\mathbf{q}) = 4\pi \sum_{lm} i^l Y_{lm}(\hat{\mathbf{q}}) C_{lm}(\mathbf{q}),$$
$$C_{lm}(\mathbf{q}) = \frac{i^{-l}}{4\pi} \int d\mathbf{q}' \rho(\mathbf{q}') Y_{lm}(\hat{\mathbf{q}}').$$

Where Y_{lm} are the spherical harmonics. An analogous expansion of $\mathbf{j}$ can be performed in terms of the vector spherical harmonics[1]:

$$\mathbf{j}(\mathbf{q}) = 4\pi \sum_{Jlm} \mathbf{Y}_m^{Jl1}(\hat{\mathbf{q}}) J_{Jl}^m(\mathbf{q}),$$
$$J_{Jl}^m(\mathbf{q}) = \frac{1}{4\pi} \int dq' \mathbf{j}(\mathbf{q}') \mathbf{Y}_m^{Jl1}(\hat{\mathbf{q}}').$$

In the low energy limit, the current multipoles J_{Jl}^m can be expressed in terms of the Coulomb multipoles, and of the Coulomb multipoles the dipole is the most dominant. [2]

It is thus possible to relate the full response (equation (2.2)), which can in principle be measured, to the unretarded dipole response:

$$R^{\mathrm{E1UR}}(\omega) = \sum_n |\langle n| D_z(\omega) |0\rangle|^2 \delta(E_n - (E_0 + \omega)). \tag{2.3}$$

For this reason we can consider the unretarded dipole (E1UR) cross section:

$$\sigma_\gamma^{\mathrm{E1UR}}(\omega) = \mathscr{G}\omega R^{\mathrm{E1UR}}(\omega),$$

where D_z refers to the unretarded dipole operator $D_z = \sum_{i=1}^A \mathbf{r}_i \tau_i^z/2$. Unretarded refers to the neglect of relativistic effects. From now on when referring to the photonuclear cross section, I shall be referring to the E1UR approximation.

[1] If unfamiliar with the vector spherical harmonics, one can find definitions and lists of properties in [18]

[2] This is called the Siegert theorem, a full derivation can be found in [19].

2.2.1 Photonuclear Moments and Sum Rules

We define the moments of the photonuclear cross section, labeled by k, as

$$m_k = \int_{\omega_{th}}^{\infty} d\omega \omega^k \sigma_\gamma^{\mathrm{E1UR}}(\omega),$$

where ω_{th} is the smallest frequency where photoabsorption is allowed (due to energy conservation). Applying the definitions from the previous section we have:

$$m_k = \mathscr{G} \sum_n |\langle n| D_z |0\rangle|^2 (E_n - E_0)^{k+1}. \tag{2.4}$$

Various ways of evaluating the sum over final states will result in expressions generally referred to as sum rules. In particular, we will consider three sum rules: the Thomas-Reiche-Kuhn (TRK), bremsstrahlungs (BSR), and polarizability sum rule (PSR) given respectively by

$$\begin{aligned}
\Sigma^{TRK} &= m_0 = \frac{\mathscr{G}}{2} \langle 0| [D,[H,D]] |0\rangle, \\
\Sigma^{BSR} &= m_{-1} = \mathscr{G} \langle 0| D_z^\dagger D_z |0\rangle, \\
\Sigma^{PSR} &= m_{-2} = \mathscr{G} \sum_n \frac{|\langle n| D_z |0\rangle|^2}{E_n - E_0}.
\end{aligned}$$

Derivations of the first two equations can be found in the Appendix section A.1.1 and A.2.1.

In the next section we will interpret the above sum rules in terms of other nuclear observables.

2.3 Sum Rules and Nuclear Observables

To handle the sum over final states in the expressions for the photonuclear sum rules (2.4), one takes advantage of the closure relation:

$$\sum_n |n\rangle \langle n| = 1.$$

By performing this analysis, we can connect the sum rules to various nuclear observables. We will briefly go over some of the results here; complete derivations

are provided in Appendix A.

2.3.1 Polarizability Sum Rule

We now refer back to the discussion in section 2.1 and see that evidently

$$\Sigma^{PSR} = 2\pi^2 \alpha_E,$$

so that calculation of the sum rule amounts directly to calculation of the electric polarizability.

In order to avoid the sum over final states, we can rewrite the sum rule (as shown in A.3.1)

$$\Sigma^{PSR} = -\mathscr{G} \langle 0| \frac{D_z^\dagger D_z}{E_0 - H} |0\rangle . \tag{2.5}$$

In later chapters, we will see how to compute the right hand side of (2.5) by using the Lanczos algorithm.

2.3.2 Thomas-Reiche-Kuhn Sum Rule

The TRK sum rule is defined by

$$\Sigma^{TRK} = \frac{\mathscr{G}}{2} \langle 0| [D,[H,D]] |0\rangle . \tag{2.6}$$

We can split the Hamiltonian in (2.6) into a kinetic and potential energy part:

$$\Sigma^{TRK} = \frac{\mathscr{G}}{2} \left(\langle 0| [D_z,[T,D_z]] |0\rangle + \langle 0| [D_z,[V,D_z]] |0\rangle \right).$$

The kinetic energy part can be explicitly calculated (A.1.2):

$$\frac{\mathscr{G}}{2} \langle 0| [D_z,[T,D_z]] |0\rangle = \mathscr{G} \frac{NZ}{2mA},$$

so that we can write

$$\Sigma^{TRK} = \mathscr{G} \frac{NZ}{2mA} \left(1 + \kappa^{TRK}\right),$$

where

$$\kappa^{TRK} = \frac{2mA}{NZ} \langle 0 | [D_z, [V, D_z]] | 0 \rangle .$$

The TRK sum rule thus allows for a computation of κ^{TRK}, known as the TRK enhancement factor, which is a measure of how much the potential does not commute with the dipole operator. If the potential has derivatives or isospin-dependent terms, then it will not commute with D_z. For a purely central potential (i.e. V = V($\mathbf{r}$)), κ^{TRK} is zero. The TRK enhancement factor is of purely theoretical interest and is a useful comparison of different potential models.

2.3.3 Bremstrahlungs Sum Rule

The BSR sum rule is defined as

$$\Sigma^{BSR} = \mathscr{G} \langle 0 | D_z^\dagger D_z | 0 \rangle .$$

There are a number of interesting ways to relate the BSR sum rule to geometric properties of the nucleus. In particular, we can show (A.2.2):

$$\Sigma^{BSR} = \mathscr{G} \left(\frac{NZ}{A} \right)^2 \langle R_{PN}^2 \rangle , \tag{2.7}$$

where $\mathbf{R}_{PN}$ is the distance between the proton and neutron centres of mass.

We define $\langle r_p^2 \rangle$ to be the mean square proton radius with respect to the nuclear centre of mass, and $\langle r_{pp}^2 \rangle$ to be the mean square distance between protons. We can show that (see A.2.3):

$$\Sigma^{BSR} = \mathscr{G} \left(Z^2 \langle r_p^2 \rangle - \frac{Z(Z-1)}{2} \langle r_{pp}^2 \rangle \right) .$$

An identical derivation can be done for neutrons (A.2.4):

$$\Sigma^{BSR} = \mathscr{G} \left(N^2 \langle r_n^2 \rangle - \frac{N(N-1)}{2} \langle r_{nn}^2 \rangle \right) . \tag{2.8}$$

Also, if we let $\langle r_{pn}^2 \rangle$ be the mean square distance between protons and neutrons we

can show (A.2.5):

$$\Sigma^{BSR} = \mathscr{G}\frac{NZ}{2}\left(\left\langle r_{pn}^2\right\rangle - \left\langle r_p^2\right\rangle - \left\langle r_n^2\right\rangle\right). \tag{2.9}$$

Finally, if $\left\langle r_p'^2\right\rangle$ is the mean square distance of protons from the proton centre of mass, we have (A.2.6):

$$\Sigma^{BSR} = \mathscr{G}\left(Z^2\left\langle r_p^2\right\rangle - Z^2\left\langle r_p'^2\right\rangle\right). \tag{2.10}$$

Chapter 3

Computational Techniques

As evidenced by the formulas in the previous chapter, calculating photonuclear sum rules requires computing the nuclear ground state, as well as applying the dipole operator. In order to do this we need a concrete representation of the ground state, which we compute by expanding in a particular basis and solving the Schrödinger equation. In practice, we use a truncated model space to compute our observables. By expanding the model space and repeating the calculations we can examine the convergence behaviour. The quality of convergence can be used to characterise the theoretical errors of our calculations.

For $A = 3,4$ nuclei, the No Core Shell Model (NCSM) has been used to calculate some of the observables we are looking at [10]. The standard NCSM is based on a harmonic oscillator basis, which has a Gaussian tail, and thus it is hard for this method to converge rapidly for nuclei with long tails, like halo nuclei. We are interested in computing observables for $A = 6,7$ nuclei including the halo nucleus ^{6}He, so we use a basis built on the hyperspherical harmonic basis which has the correct exponential asymptotic behaviour built in.

3.1 Hyperspherical Basis

The Hyperspherical formalism is based on a generalization of the standard solution to the two-body problemin which you you move to the center of mass frame and consider a single body with relative coordinates and reduces mass. The hy-

perspherical coordinates are built up from the Jacobi coordinates(see section B.1), which remove the centre of mass motion and consider $A-1$ radial coordinates with $2(A-1)$ corresponding polar angles. Using the radial Jacobi coordinates η_i, we construct a hyper-radial coordinate ρ related to the "size" of the system:

$$\rho_k{}^2 = \sum_{i=1}^{k} \eta_i{}^2 = \frac{1}{k} \sum_{i<j}^{k+1} (\mathbf{r}_i - \mathbf{r}_j)^2 .$$

and through a recursive process generate $A-2$ hyper-angles φ_i, which correspond to polar angles in and abstract $3(A-1)$ dimensional space.

By transforming the Laplace operator into hyperspherical coordinates we find

$$\Delta = \frac{\partial^2}{\partial \rho^2} + \frac{3(A-1)-1}{\rho} \frac{\partial}{\partial \rho} - \frac{1}{\rho^2} \widehat{K}^2,$$

where $\widehat{K}$ is an operator that depends on the angles and hyper-angles but not the hyper-radius. One interprets $\widehat{K}$ to be a generalization of the angular momentum operator $\widehat{l}$, and we refer to khat as the grandangular momentum operator. More details are provided in Appendix B.

Using these coordinates, we can construct the hyperspherical basis $R_\nu(\rho) H_K(\Omega)$, where $H_K(\Omega)$ is made by the eigenstates of $\widehat{K}^2$, called the hyperspherical harmonics. The $H_K(\Omega)$ must be constructed to be antisymmetric since we are working with fermions.

3.2 Evaluation of Matrix elements

One of the advantages of using an antisymmetrized hyperspherical basis is the way we can simplify matrix elements. With any totally antisymmetrized states $|\psi\rangle$, $|\psi'\rangle$ and a one-body operator $O_{(1)} = \sum_{i=1}^{A} O_i$, we can reduce the matrix element to that of an operator that acts on only one particle:

$$\langle \psi | O_{(1)} | \psi \rangle = A \langle \psi | O_A | \psi \rangle .$$

Similarly, for a two-body operator $O_{(2)} = \sum_{i<j}^{A} O_{ij}$, we can write the matrix element as

$$\langle \psi | O_{(2)} | \psi' \rangle = \frac{A(A-1)}{2} \langle \psi | O_{A,A-1} | \psi' \rangle .$$

In the case of one-body operators, we note that when we use Jacobi coordinates, that last coordinate η_{A-1} is proportional to the position of the last particle with respect to the centre of mass of the system:

$$\eta_{A-1} = \sqrt{\frac{A}{A-1}} \mathbf{r}'_A .$$

And in fact the last Jacobi coordinate is also proportional to the hyper-radius ρ:

$$\eta_{A-1} = \rho \sin \varphi_{A-1} .$$

If we have the matrix element of a one body operator $O_{(1)}$, we can write it in terms of an operator that acts only on the last particle, and so in terms of the magnitude, direction, and spin-isospin components of the last particle coordinates:

$$\langle \psi | O_{(1)} | \psi \rangle = A \langle \psi | O_A | \psi \rangle = A \langle \psi | O(r'_A, \hat{r}'_A, \sigma_A, \tau_A) | \psi' \rangle ,$$

where now we can replace r'_A above with $\sqrt{\frac{A-1}{A}} \rho_{A-1} \sin(\varphi_{A-1})$.

The spin-angular and isospin portions of the matrix element can now be calculated analytically using standard angular momentum methods. The hyper-angular and hyper-radial portions of the matrix element are reduced to two one-dimensional integrals since the wavefunction $|\psi\rangle$ and $|\psi'\rangle$ are both expanded in terms of the hyperspherical basis, which are products of hyper-radial and hyper-angular functions. The details of these final integrals are left out and can be found in [20] and [19]. In practice, we have used Gaussian Quadrature to compute these integrals numerically.

Now let us consider two-body operators. We can write two-body matrix elements in terms of the last two particles matrix elements only,

$$\langle \psi | O_{(2)} | \psi' \rangle = \frac{A(A-1)}{2} \langle \psi | O_{A,A-1} | \psi' \rangle .$$

If our operator only cares about the particle relative position and spin-isospin (for example, a central potential), then

$$\frac{A(A-1)}{2}\langle\psi|O_{A,A-1}|\psi'\rangle = \frac{A(A-1)}{2}\langle\psi|O(r'_A - r'_{A-1},\sigma_A,\sigma_{A-1},\tau_A,\tau_{A-1})|\psi'\rangle.$$

Then we can use the reverse-choice for our Jacobi coordinates, i.e. we choose the last Jacobi coordinate η_{A-1} as pointing between the last two particles,

$$\eta_{A-1} = \sqrt{\frac{1}{2}}(\mathbf{r'_A} - \mathbf{r'_{A-1}}),$$

then η_{A-2} points between the third-to-last particle and the centre of mass of the last two, and so on. Then we have:

$$\langle\psi|O_{(2)}|\psi'\rangle = \frac{A(A-1)}{2}\langle\psi|O(\sqrt{2}\rho_{A-1}\sin(\varphi_{A-1},\hat{\eta}_{A-1},\sigma_A,\sigma_{A-1},\tau_A,\tau_{A-1})|\psi'\rangle.$$

Using very similar ideas to those in the previous section, we can write the matrix element as a sum of products of hyper-radial/hyper-angular, spin-angular and isospin parts. The later two are again calculable analytically, while the former is again reduced to two one-dimensional integrals which can be computed numerically.

3.3 The Lanczos Algorithm

The Lanczos algorithm is used to tridiagonalize matrices, i.e. to convert them to the following form:

$$H = \begin{bmatrix} a_0 & b_1 & 0 & 0 & \dots \\ b_1 & a_1 & b_2 & 0 & \dots \\ 0 & b_2 & a_2 & b_3 & \ddots \\ 0 & 0 & b_3 & a_3 & \ddots \\ \vdots & \vdots & \ddots & \ddots & \ddots \end{bmatrix}$$

by recursively generating an orthonormal set of vectors $\{|\phi_i\rangle\}$.

Tridiagonalization routines are commonly used to simplify hermitian matrices because there are very efficient algorithms for computing eigenvalues and eigen-

vectors of tridiagonal matrices. The Lanczos algorithm in particular has the property that even when applied to a truncated linear operator on an infinite dimensional Hilbert space, the eigenvalues of the resulting finite matrix approach the eigenvalues of the original operator. This makes it a useful tool for tridiagonalizing the Hamiltonian and computing the ground state energy in a truncated model space.

In addition to this useful feature, we have a simple recursive expression for the determinant of a tridagonal matrix:

$$\det(H) = a_0 \det[H]_{\{2,\ldots,n\}} - b_1^2 \det[H]_{\{3,\ldots,n\}} \tag{3.1}$$

where $[H]_{2,\cdots,n}$ is the matrix made from the 2^{nd} to n^{th} columns and rows of H. This property will be used in section 3.4.1 to derive the closed form expression for the polarizability sum rule.

To formulate the algorithm, suppose we start with a matrix H. First, a vector of unit length must be chosen for $|\phi_0\rangle$. In general one can try to choose a starting vector in such a way as to optimize convergence, but in our case we make a particular choice of $|\phi_0\rangle$ for analytic reasons which will be described in the following sections. Once $|\phi_0\rangle$ is selected, the others are calculated recursively by

$$b_{i+1} |\phi_{i+1}\rangle = H |\phi_i\rangle - a_i |\phi_i\rangle - b_i |\phi_{i-1}\rangle . \tag{3.2}$$

where

$$\begin{aligned} |\phi_{-1}\rangle = 0, \qquad & \langle \phi_i | \phi_j \rangle = \delta_{ij}, \\ a_0 = \langle \phi_0 | H |\phi_0\rangle \qquad & , b_0 = 0. \end{aligned}$$

We can see from (3.2) that

$$\langle \phi_j | H |\phi_i\rangle = \langle \phi_j | \left(b_{i+1} |\phi_{i+1}\rangle + a_i |\phi_i\rangle + b_i |\phi_{i-1}\rangle \right) = \begin{cases} b_i & j = i-1 \\ a_i & j = i \\ b_{i+1} & j = i+1 \\ 0 & \text{otherwise} \end{cases}$$

and thus, in the basis formed by the Lanczos vectors, H is tridiagonal with coeffi-

cients a_i and b_i (called Lanczos coefficients).

3.4 Implementation

Given the form of the sum rules derived above, we see that there are three fundamental computational tasks which must be performed to calculate them. The first is calculation of the nuclear ground state $|0\rangle$, which entails solving the Schrödinger equation and requires calculating matrix elements of the form

$$H_{KK'\nu\nu'} = \langle K| \langle \nu| H \left|K'\right\rangle \left|\nu'\right\rangle,$$

where here we identify $|K\rangle$, $|\nu\rangle$ with the hyper-angular-spin-isospin and hyperradial parts of the hyperspherical harmonic basis states, respectively.

As is the case with most algorithms for solving for eigenvalues and eigenvectors of hermitian matrices, the Hamiltonian is first trigiagonalized, for which the Lanczos algorithm is used.

The number of matrix elements that need to be calculated can be limited by choosing only those basis states which share quantum numbers with the states of interest. In particular, for the ground state we only compute matrix elements for basis states with total angular momentum, isospin, and isospin projection (J,T,T_z) equal to that of the ground state. The hyperspherical harmonics are all characterized by a grandangular moment quantum number K. We control the size of our model space by generating all states with the correct J,T,T_z quantum numbers and K less than or equal to some maximum number $K_{\max}$. Then, by increasing $K_{\max}$, we can assess the truncation error of our calculations.

We also have to multiply the Hamiltonian by the Lanczos vectors $\left|\phi^i\right\rangle$ as part of the Lanczos algorithm, which corresponds to calculating

$$\phi^{n+1}_{K\nu} = \sum_{K'\nu'} H_{KK'\nu\nu'}\phi^n_{K'\nu'} - a_n\phi_{K\nu} - b_n\phi^{n-1}_{K\nu},$$

where $\phi^n_{K\nu} = \langle K| \langle \nu| |\phi^n\rangle$. As this computation must be performed for every Lanczos vector (the number of which is determined by the number of basis states used), this is the most computationally intensive part for the larger model spaces. This is the algorithm that I focused on parallelizing.

Finally, we also have to compute $\langle 0| D_z^\dagger D_z |0\rangle$. To do this we must expand D_z $|0\rangle$ by generating the basis states with the quantum numbers determined by the selection rules for D_z, namely $\Delta J = 1$, $\Delta T = 1$, and $\Delta T_z = 0$. So, for the case of ^{4}He, where in the ground state $J = 0, T = 0, T_z = 0$, we would need to generate states for $D_z\,|0\rangle$ with quantum numbers $J = 1, T = 1, T_z = 0$.

In general there will be multiple transition channels. In particular for the case of ^{6}He we have for the ground state ($J = 0, T = 1, T_z = -1$), and so we have two transition channels ($J = 1, T = 1, T_z = -1$) and ($J = 1, T = 2, T_z = -1$). The computations must be performed for each channel and then the results combined to calculate the sum rules. This is described in more detail in later sections.

These main computational tasks are performed by a code written by Barnea and Novoselsky (referred to henceforth as the HH code), which computes completely antisymmetrized hyperspherical basis states and computes Lanczos coefficients [21, 22]. I wrote a code from scratch that combined these raw elements into calculated values for the sum rules. The details of this sum rule computation is presented in the next subsection.

3.4.1 Calculating the Sum Rules

Recall equation (2.5):

$$\Sigma^{PSR} = -\mathscr{G}\,\langle 0|\,\frac{D_z^\dagger D_z}{E_0 - H}\,|0\rangle\,.$$

We rewrite this as

$$\Sigma^{PSR} = -\mathscr{G}\,\langle 0| D_z^\dagger D_z |0\rangle\,\langle \phi_0|\,\frac{1}{E_0 - H}\,|\phi_0\rangle\,,$$

where $|\phi_0\rangle = \frac{D_z|0\rangle}{\sqrt{\langle 0|D_z^\dagger D_z|0\rangle}}$, which is by construction of unit length. Let $|\phi_0\rangle$ be the first Lanczos vector, from which the complete set $\{|\phi_i\rangle\}$ are recursively defined. Then define $x_{nm} = \langle \phi_n|\,\frac{1}{E_0 - H}\,|\phi_m\rangle$. Clearly

$$|\phi_0\rangle = (E_0 - H)\,\frac{1}{E_0 - H}\,|\phi_0\rangle\,.$$

which we can write component-wise as

$$\sum_n (E_0 - H_{mn}) x_{n0} = \delta_{m0},$$

where δ_{ij} is the Kronecker delta function. Using Cramer's Rule for linear systems, we have

$$x_{00} = \frac{\det([E_0 - H]_{\{2,\cdots,n\}})}{\det(E_0 - H)}.$$

By definition, H is tridiagonal in the $|\phi_i\rangle$ basis, so clearly $E_0 - H$ is also tridiagonal. Thus we can apply the recursive formula for the determinant of a tridiagonal matrix (3.1), the end result of which (in terms of the Lanczos coefficients a_i, b_i is

$$x_{00} = \cfrac{1}{E_0 - a_0 - \cfrac{b_1^2}{E_0 - a_1 - \cfrac{b_2^2}{E_0 - a_2 - \cfrac{b_3^2}{\cdots}}}}.$$

This continued fraction is very fast to compute given the Lanczos coefficients and converges quickly with the number of Lanczos coefficients (in practice the first 1000 terms is more than sufficient to converge to machine precision). The Lanczos coefficients are calculated by the HH code as part of the Lanczos algorithm, and are then used as an input to my code.

Finally, we have a number for the polarizability sum rule:

$$\Sigma^{PSR} = -\mathscr{G} \langle 0 | D_z^\dagger D_z | 0 \rangle x_{00}.$$

In practice, for ^{6}He we have two transition channels which will each produce a set of Lanczos coefficients. The results is the sum over each channel:

$$\Sigma^{PSR} = -\mathscr{G} \sum_T \langle 0 | D_z^\dagger D_z | 0 \rangle^T x_{00}^T. \tag{3.3}$$

For the TRK sum rule we have:

$$\begin{aligned}
\Sigma^{TRK} &= \mathscr{G} \sum_n \langle 0| D_z^\dagger |n\rangle \langle n| D_z |0\rangle (E_n - E_0), \\
&= \mathscr{G} \sum_n \langle 0| D_z^\dagger E_n |n\rangle \langle n| D_z |0\rangle - \langle 0| D_z^\dagger |n\rangle \langle n| D_z |0\rangle E_0, \\
&= \mathscr{G} \left(\langle 0| D_z^\dagger H D_z |0\rangle - \langle 0| D_z^\dagger D_z |0\rangle E_0 \right), \\
&= \mathscr{G} \langle 0| D_z^\dagger D_z |0\rangle (\langle \phi_0| H |\phi_0\rangle - E_0), \\
&= \mathscr{G} \langle 0| D_z^\dagger D_z |0\rangle (a_0 - E_0).
\end{aligned}$$

where $|\phi_0\rangle$ is defined as before. Thus we can calculate Σ^{TRK} using $\langle 0| D_z^\dagger D_z |0\rangle$ and the first Lanzcos coefficient.

In the case of multiple transitions channels:

$$\Sigma^{TRK} = \mathscr{G} \sum_T \langle 0| D_z^\dagger D_z |0\rangle^T \left(a_0^T - E_0 \right). \tag{3.4}$$

The BSR sum rule is given simply by

$$\Sigma^{BSR} = \mathscr{G} \langle 0| D_z^\dagger D_z |0\rangle,$$

or

$$\Sigma^{BSR} = \mathscr{G} \sum_T \langle 0| D_z^\dagger D_z |0\rangle^T. \tag{3.5}$$

in the case of multiple channels.

Equations (3.3), (3.4), (3.5) therefore allow us to compute the sum rules given the Lanzcos coefficients and the value of $\langle 0| D_z^\dagger D_z |0\rangle$ produced by the HH code.

Chapter 4

Calculating the Full Continuum Response

The methods described in the previous chapters used the Lanczos technique to calculate the moments of the photonuclear cross section without resorting to computing the full continuum response. This response can be computed, however, using a Lorentz Integral transform method. Since some of these cross sections are available from previous work [3], it will be interesting to check our results from the computation of sum rules with the results from direct integration of the cross section, using the definition of the moments:

$$m_k = \int_{\omega_{th}}^{\infty} d\omega \omega^k \sigma_\gamma^{\mathrm{E1UR}}(\omega).$$

The Lorentz Integral Transform of the response function (equation (2.3)) is defined:

$$\mathscr{L}(\sigma) = \int d\omega \frac{R(\omega)}{(\omega - \sigma_R)^2 + \sigma_I^2},$$

where $\sigma = \sigma_R + i\sigma_I$.

Plugging in the form of the response, we have:

$$\begin{aligned}\mathscr{L}(\sigma) &= \int d\omega \int dn \frac{|\langle n| D_z |0\rangle|^2 \, \delta(E_n - E_0 - \omega)}{(\omega - \sigma_R)^2 + \sigma_I^2}, \\ &= \int d\omega \int dn \frac{\langle 0| D_z^\dagger |n\rangle \langle n| D_z |0\rangle \, \delta(E_n - E_0 - \omega)}{(\omega - \sigma_R)^2 + \sigma_I^2}, \\ &= \int dn \frac{\langle 0| D_z^\dagger |n\rangle \langle n| D_z |0\rangle}{(E_n - E_0 - \sigma_R)^2 + \sigma_I^2}.\end{aligned}$$

Now it is useful to expand

$$(E_n - E_0 - \sigma_R)^2 + \sigma_I^2 = (E_n - E_0 - \sigma_R + i\sigma_I)(E_n - E_0 - \sigma_R - i\sigma_I),$$

and, using the fact that $E_n |n\rangle = H |n\rangle$, we can apply the closure relation to derive:

$$\begin{aligned}\mathscr{L}(\sigma) &= \langle 0| D_z^\dagger \left(\frac{1}{H - E_0 - \sigma_R + i\sigma_I} \right) \left(\frac{1}{H - E_0 - \sigma_R - i\sigma_I} \right) D_z |0\rangle, \\ &= \frac{1}{\sigma_I} \mathrm{Im} \left[\langle 0| D_z^\dagger \left(\frac{H - E_0 - \sigma_R + i\sigma_I}{H - E_0 - \sigma_R + i\sigma_I} \right) \left(\frac{1}{H - E_0 - \sigma_R - i\sigma_I} \right) D_z |0\rangle \right], \\ &= \frac{1}{\sigma_I} \mathrm{Im} \left[\langle 0| D_z^\dagger \left(\frac{1}{H - E_0 - \sigma_R - i\sigma_I} \right) D_z |0\rangle \right], \\ &= -\frac{1}{\sigma_I} \mathrm{Im} \left[\langle 0| D_z^\dagger \left(\frac{1}{E_0 + \sigma_R + i\sigma_I - H} \right) D_z |0\rangle \right], \\ &= -\frac{1}{\sigma_I} \mathrm{Im} \left[\langle 0| D_z^\dagger \left(\frac{1}{z - H} \right) D_z |0\rangle \right].\end{aligned}$$

where $z = E_0 + \sigma_R + i\sigma_I$.

Now we can apply an argument analagous to section 3.4.1 by setting

$$|\phi_0\rangle = \frac{D_z |0\rangle}{\sqrt{\langle 0| D_z^\dagger D_z |0\rangle}},$$

so that we can write

$$\mathscr{L}(\sigma) = -\frac{1}{\sigma_I} \langle 0| D_z^\dagger D_z |0\rangle \, \mathrm{Im} \left[\langle \phi_0 | \frac{1}{z-H} | \phi_0 \rangle \right],$$

$$\mathscr{L}(\sigma) = -\frac{1}{\sigma_I} \langle 0| D_z^\dagger D_z |0\rangle \, \mathrm{Im} \left[\cfrac{1}{z - a_0 - \cfrac{b_1^2}{z - a_1 - \cfrac{b_2^2}{z - a_2 - \cfrac{b_3^2}{\cdots}}}} \right].$$

Where again a_i, b_i are the Lanczos coefficients.

Inverting the transform $\mathscr{L}(\sigma)$ to obtain $R(\omega)$ is a numerical task accomplished by fitting the transformed response function to an easily transformable ansatz with many parameters. Thus the full response can be calculated from the same Lanczos coefficients used in the sum rule computations.

As mentioned above, some cross sections calculated with this method are available for ^{6}He from [**?**]. I have used these cross sections to extract values for the photonuclear moments by direct integration which can be compared with the sum rule calculation. The difference between this method and the direct computation of the sum rules is that one has to go through the inversion procedure, which introduces additional numerical errors.

Chapter 5

Results

5.1 Testing the Sum Rule Code

To test my sum rule code, I compared results from Gazit et al. [1], which performed these sum rule calculations for ^{4}He using the AV18-UIX potentials. Their result at various sizes of model space are shown in Table 5.1, compared to my results computing the sum rules using the same Lanzcos coefficients. The values agree to within what can be attributed to machine precision.

As a next step, I calculated the polarizability sum rule for ^{4}He using the same simple potentials that I would be using for ^{6}He: the Minnesota (MN) [23, 24], Argonne V4' (AV4') [25], and the Malfiet-Tjon I-III (MT13) [26]. The x-axis denotes the maximum grandangular momentum of the basis states used for the

	PSR		BSR		TRK	
$K_{\max}$	[1]	This work	[1]	This work	[1]	This work
16	0.06434	0.06434	2.406	2.405	146.0	145.9
18	0.06473	0.06473	2.410	2.409	146.2	146.2

Table 5.1: Previous calculations from Gazit et al. [1] of the sum rules using the Lanzcos coefficients are compared with our calculations using the same Lanzcos coefficients to test the validity of the sum rule code. We compared our results for largest model spaces denoted by $K_{\max}$.

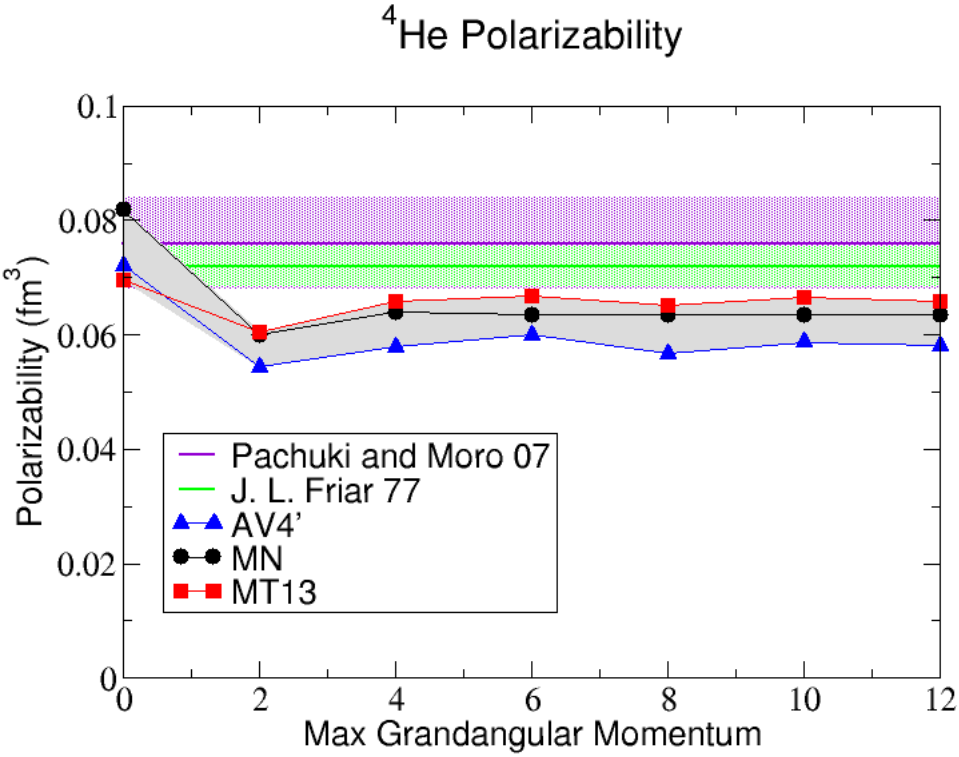

Figure 5.1: Polarizability of ^{4}He computed using different sized model spaces denoted by maximum grandangular momentum $K_{\max}$. The experimental points were obtained by Compton scattering with experimental error indicated by the shaded regions.

calculation. As discussed in the Chapter 3, the maximum grandangular momentum is allowed to vary as a way to assess the error due to truncation of our model space. States with even grandangular momentum K have even parity, so for the ground state we used even $K_{\max}$, which is why points appear on the plot in increments of two. In fact we are also generating states up to $K = K_{\max} + 1$, since the dipole operator carries odd parity, so the odd $K_{\max} + 1$ states are needed to expand $D_z |0\rangle$. Thus, I will refer to model space sizes as $K_{\max} = X/X + 1$ for even X, to reflect the states used to expand $|0\rangle / D_z |0\rangle$.

The values appear fairly well converged in $K_{\max}$. We can estimate the trun-

	Convergence Error
MN	1.0%
AV4'	0.1%
MT13	1.1%

Table 5.2: Convergence error in the polarizability sum rule for ^{4}He with the simple potential models. The value is estimated as the percentage change from the $K_{\max} = 10$ to $K_{\max} = 12$ model space size.

Theory		Experiment	
0.06830(8)(14)	[10]	0.072(4)	[2]
0.0655(4)	[1]	0.076(8)	[27]
0.0635(4)	This work		

Table 5.3: Theoretical and experimental results for the polarizability of ^{4}He. The two other theoretical values were computed using more realistic two-body potential models and included three-body forces. The experimental values were obtained through Compton scattering.

cation error by taking the percentage change in the last two points, which we summarize in Table 5.2. There is clearly a non-negligible potential dependence in the theoretical results shown in Figure 5.1. For this reason, we take as our best value the average of the three results in the largest model space, using their standard deviation as the error. The value is compared with existing theoretical and experimental results in Table 5.3. Note that the result from [10] and [1] include realistic two-body forces and three-body forces, whereas ours have neither. These factors both help the comparison with experiment. The deviation of our calculations from the experimental data are not large, but they are also not unexpected, as the semi-realistic potentials used are only expected to reproduce the bulk of the nuclear dynamics and not the details.

5.2 Parallelization

The version of the HH code I started with was a serial code, only able to run on a single processor. This is not a problem for the ^{4}He calculations, but the number of

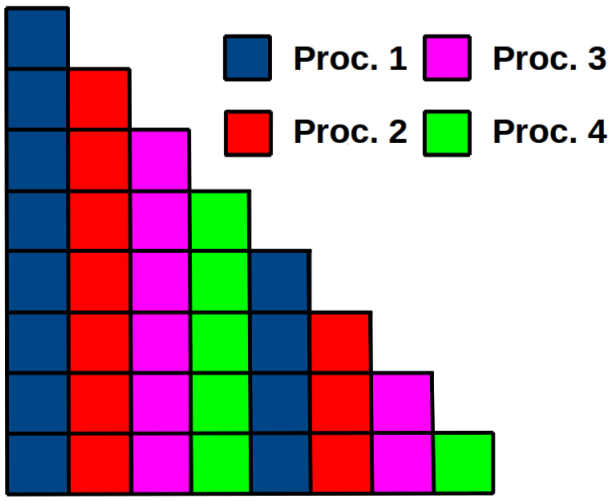

Figure 5.2: A cartoon of how the matrix elements in a hermitian matrix can be allocated efficiently between four processors. The colour of each matrix element corresponds to the processor it is assigned to.

hyperspherical harmonics becomes large when $A > 4$, meaning calculations take much longer for ^{6}He. In the interest of saving computation time, I attempted to parallelize the part of the code which multiplied a Lanczos vector by the Hamiltonian matrix (recall equation (3.2)), as this is the most significant bottleneck for large model spaces[1].

The parallel algorithm splits the columns of the Hamiltonian matrix and the corresponding components of the vector among the processors in an efficient way and then allows the results to be collected and summed together for the final answer. Since the Hamiltonian is hermitian, only the upper or lower triangular elements needed to be considered, which meant the effective size of each column was not constant. The simplest method we used was going through the columns in order while rotating the processor which it would be assigned to. So, for instance, (with four processors) the n^{th} processor would be assigned all columns numbered n modulo 4. See Figure 5.2 for a illustration.

The implementation of the parallel algorithm was done using the Message

[1] Some other parts of the code had already been parallelized.

Passing Interface (MPI) and run on the TRIUMF Theory Cluster known as cougar[2]. An actual speed up of computation time was achieved. The magnitude of the speed up will depend greatly on the computation that is being done, since certain parts of the code are parallelized more efficiently than others and the location of the bottleneck can depend on the nature of the input. Since the focus of the parallelization was the Hamiltonian multiplication in the Lanczos Algorithm, the parallel code is expected to do better with larger Hilbert spaces. For an intermediate sized space using $K_{\max} = 6/7$ (corresponding to a matrix dimension of 10^4) and the MN potential, I was able to observe a decrease in time from about 170 minutes to just over 17 minutes when running on 12 processors, leading to a speed up factor of 10.

5.3 Sum Rules

We have calculated all three of the sum rules for ^{6}He using the three semi-realistic potentials we used for ^{4}He. The results for the TRK, BSR, and Polarizability sum rules are plotted in Figures 5.3, 5.4, and 5.5 respectively. We identify two sources of theoretical error, a convergence error and a model dependent error. The convergence error is the error due to the truncation of the model space; we estimate it as the percentage change between the last two model space sizes. We estimate the model dependent error as the standard deviation of the values that the three potential models give for a given sum rule.

The TRK and BSR sum rules appear better converged than the PSR. From a theoretical point of view, it is interesting to note that the AV4' potential has the largest TRK sum rule, meaning it has the largest enhancement factor. The TRK sum rule is least sensitive of the model dependence, with a spread of about 5.82%. The BSR sum rules measures the total dipole strength and happens to be bigger as well for the AV4'. The MT13 is has a more converged value for the BSR sum rule, but it is also smaller than the other two. The model dependence for the BSR sum rule is 10.1%.

The PSR presents the weakest convergence pattern. The AV4' and MN values are still growing, while only the MT13 shows a decent convergence pattern. The PSR has the largest model dependence of 31.1%. In fact, we can note that

[2]http://cougar.triumf.ca

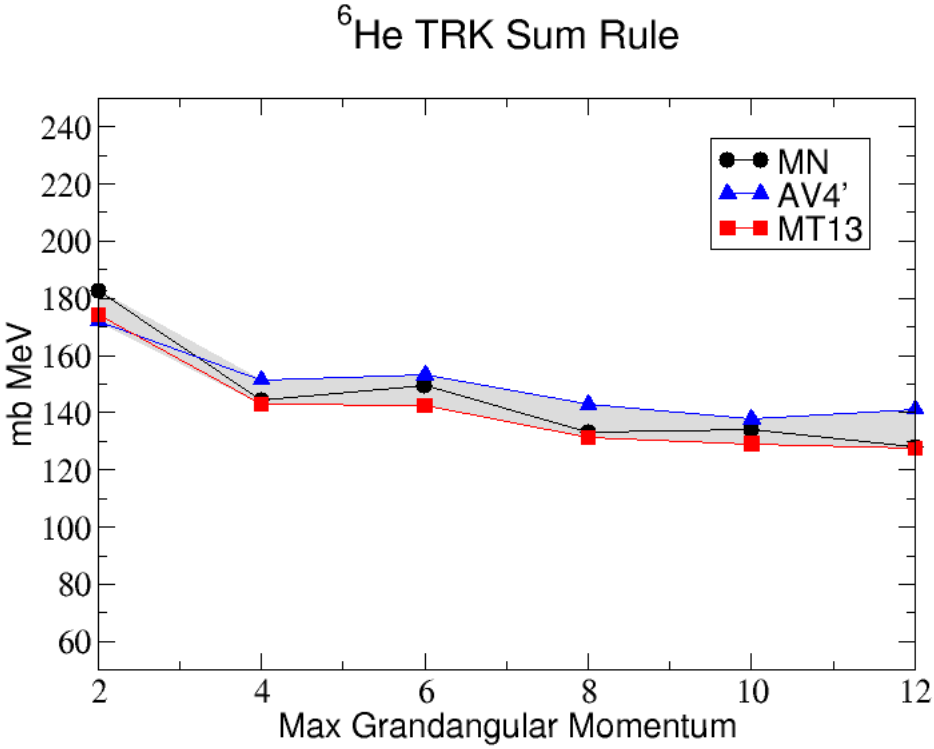

Figure 5.3: TRK sum rule computations for different sizes of model space characterized by max grandangular momentum $K_{\max}$.

the model dependence in the PSR is much larger than the same sum rule for ^{4}He using the same potentials. This is consistent with the results from [3] in which the photoabsoption cross sections were calculated: Since the PSR depends on the inverse-square energy-weighted integral of the cross section, it is most sensitive to the low-energy portion of the cross section, in particular the location of the threshold energy (Recall that the threshold energy is the minimum energy required for photoabsorption). The threshold energy of ^{4}He is about 20 MeV, while the threshold for ^{6}He is only about 1 MeV (since the neutron halo is loosely bound), so ^{6}He should be much more sensitive to the threshold energy than ^{4}He, which is where [3] found there to be the largest discrepancy between potentials. The computed values for the model dependent error and the convergence error are listed in Tables

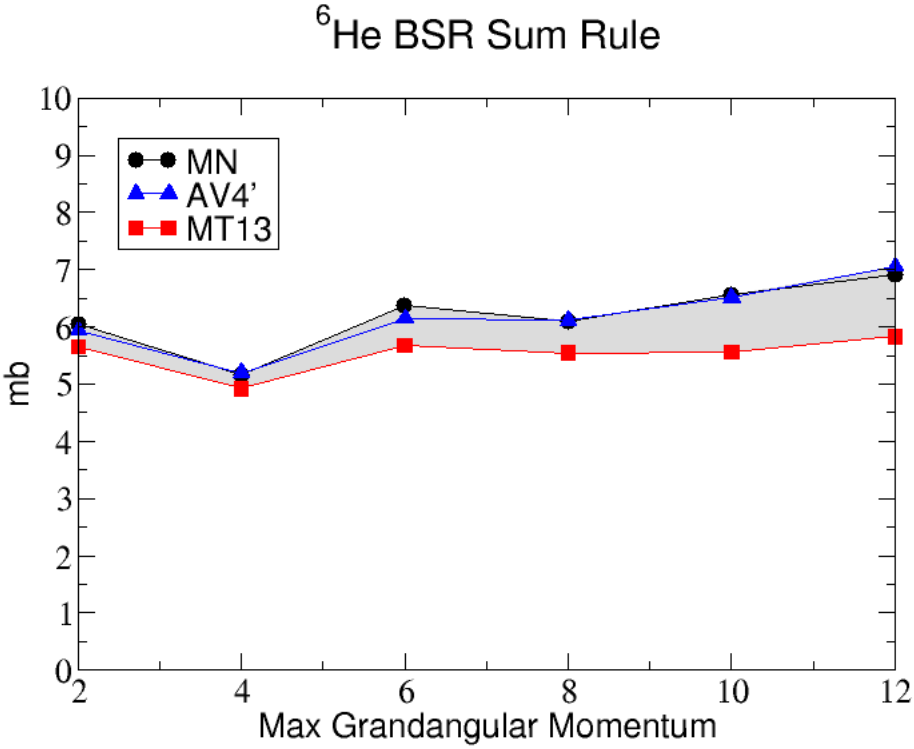

Figure 5.4: BSR sum rule computations for different size of model space characterized by max grandangular momentum $K_{\max}$.

	MN	AV4'	MT13
TRK	4.34%	2.47%	2.66%
BSR	5.27%	8.38%	4.76%
PSR	22.0%	28.3%	13.4%

Table 5.4: Convergence error estimate for sum rules. Computed as the percentage change in the value from the second-largest to the largest model space.

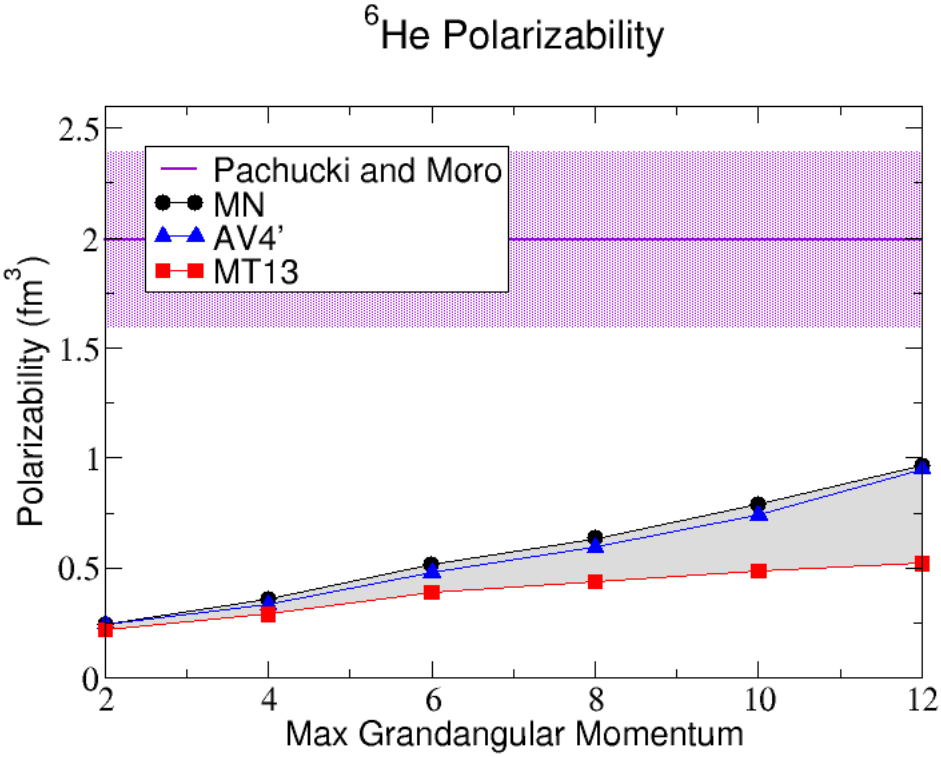

Figure 5.5: Polarizability sum rule computations for different sizes of model space characterized by max grandangular momentum $K_{\max}$. The experimental point is from Pachucki and Moro [2] using Coulomb breakup, the shaded region is the experimental error.

5.5 and 5.4 respectively. Note that even though there is non-negligible convergence error in all the sum rules, this error is still dominated by the model dependent error, as was the case for ^{4}He.

Different potential models may overbind or underbind the ground states of nuclei. We would expect that a potential that overbinds a nucleus would also compute a polarizability that is too small. In Table 5.6, I have plotted the computed binding energies using the three different potentials for the $K_{\max} = 12$ model space. This can be compared to the binding energy from the National Nuclear Data Center: -29.27. I have included the ^{4}He results as well, which can be compared to its

	Mean	Spread
TRK	132.3	5.82%
BSR	6.599	10.1%
PSR	0.812	31.1%

Table 5.5: Estimated model-dependent error. Computed as the standard deviation from the mean value among potential models used.

	BE (MeV)	r_{rms} (fm)
	^{6}He	
MN	-30.50(3)	2.42(7)
AV4'	-32.90(3)	2.38(7)
MT13	-31.81(9)	2.25(2)
	^{4}He	
MN	-23.95(1)	1.410(1)
AV4'	-32.25(36)	1.386(2)
MT13	-30.74(17)	1.422(2)

Table 5.6: Binding energies and root mean square radii for ^{6}He and ^{4}He using $K_{\text{max}} = 12$. The error in the last digit is taken to be the difference between the $K_{\text{max}} = 12$ and $K_{\text{max}} = 10$ values.

measured binding energy -28.30. We see that all our potentials overbind ^{6}He. In fact, our calculated values for the PSR are smaller than the experimental result provided by Pachucki and Moro [2] determined from Coulomb breakup of ^{6}He on lead,

5.4 Photoabsorption Cross Section

The ^{6}He photoabsorption cross sections were calculated by Bacca et al. [3] using the Lorentz Integral Transform technique discussed in chapter 4. The cross section is only computed up to some finite energy, but the integrals are required to be taken to infinity to calculate the photonuclear moments. In the case of the PSR, however, since the cross section is inverse-square energy-weighted, the tail contributes little to the value of the integral. In fact, attempting to fit the tail to a reasonable

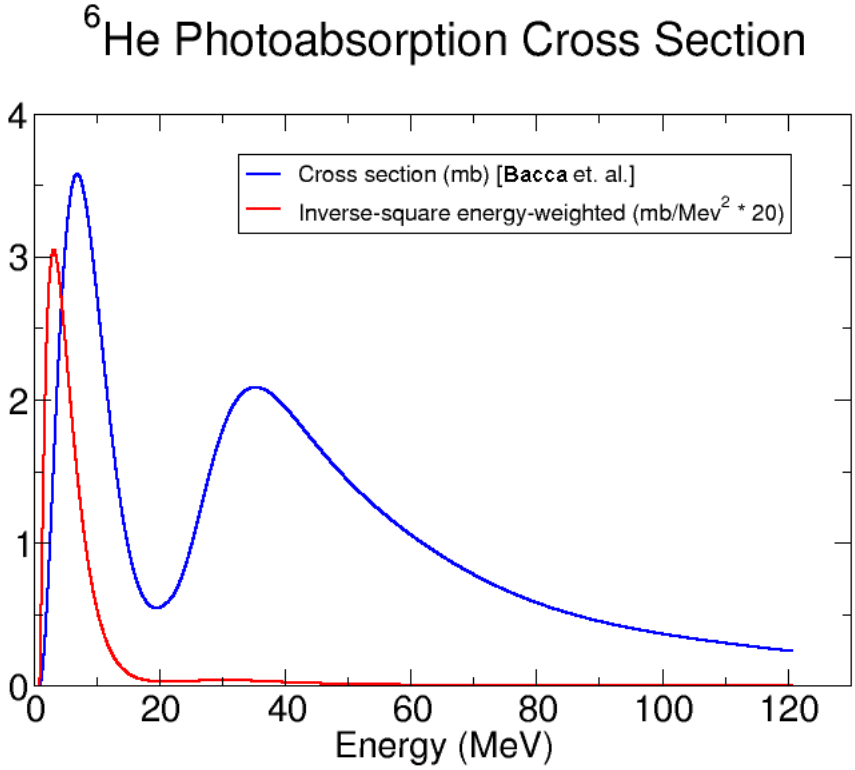

Figure 5.6: The photoabsorption cross section computed by Bacca et al. [3] using the AV4' potential. The inverse-square energy-weighted cross section is included (scaled to be visible) to show how the lack of data going to infinity does not effect the value of the PSR. The model space size used to compute the cross section was $K_{\max} = 12$.

ansatz and integrating results in a contribution on the order of 0.01%, which is significantly smaller than both the convergence and model dependent error. Figure 5.6 shows the computed cross section from [3] compared to the inverse-square energy-weighted cross section, which has been scaled to appear in the Figure.

We can use the integral of the computed cross section as another test of the sum rule computations. Since the cross section was computed with AV4' and using $K_{\max} = 12$, we can compare the integral of the inverse-square energy-weighted cross section to the sum rule calculation using the same potential and model space

Integral	Sum Rule
0.946	0.951

Table 5.7: PSR of ^{6}He calculated by integrating the cross section compared to sum rule approach.

size. This is summarized in Table 5.7. The only difference between the calculation of the cross section and the integral are the fact that the integral introduces numerical errors due to the inversion procedure which are avoided in the sum rule calculation. Thus, we can attribute a small discrepancy between these two values as due to this numerical error.

5.5 Conclusions

In this work, I present the first *ab-initio* calculation of the polarizability sum rule for ^{6}He. The calculation is performed with simple potentials as a starting point. This lays the groundwork for future, more sophisticated calculations.

The truncation of the Hilbert space still plays a large role in our computed results for the ^{6}He sum rules, i.e., the calculations are not fully converged. Evidently the dipole operator couples more strongly to high grandangular momenta of ^{6}He than ^{4}He. The values may now be beginning to converge, however, and perhaps $K = 14$ or $K = 16$ states will show reasonable convergence. These much larger Hilbert spaces can be achieved using our parallel code, but we were unable to complete the calculations due to lack of time. Certainly a proper truncation of the hyperspherical harmonics negligible symmetries to reduce the number of states will have to be used.

Bibliography

[1] D. Gazit, N. Barnea, S. Bacca, W. Leidemann, and G. Orlandini. Photonuclear sun rules and the tetrahedral configuration of he-4. *Phys. Rev. C*, 36:061001, 2006.

[2] K. Pachucki and A. M. Moro. Nuclear polarizability of helium isotopes in atomic transitions. *Phys. Rev. A*, 75(3):032521, 2007.

[3] Sonia Bacca, Mario Andrea Marchisio, Nir Barnea, Winfried Leidemann, and Giuseppina Orlandini. Microscopic calculation of six-body inelastic reactions with complete final state interaction: Photoabsorption of ^6he and ^6li. *Phys. Rev. Lett.*, 89(5):052502, Jul 2002.

[4] P. Navrátil, V. G. Gueorguiev, J. P. Vary, W. E. Ormand, and A. Nogga. Structure of $a = 10 - -13$ nuclei with two- plus three-nucleon interactions from chiral effective field theory. *Phys. Rev. Lett.*, 99(4):042501, Jul 2007.

[5] P. Mueller, I. A. Sulai, A. C. C. Villari, J. A. Alcántara-Núñez, R. Alves-Condé, K. Bailey, G. W. F. Drake, M. Dubois, C. Eléon, G. Gaubert, R. J. Holt, R. V. F. Janssens, N. Lecesne, Z.-T. Lu, T. P. O'Connor, M.-G. Saint-Laurent, J.-C. Thomas, and L.-B. Wang. Nuclear charge radius of ^8he. *Phys. Rev. Lett.*, 99(25):252501, Dec 2007.

[6] I. Tanihata, D. Hirata, T. Kobayashi, S. Shimoura, K. Sugimoto, and H. Toki. Revelation of thick neutron skins in nuclei. *Physics Letters B*, 289(3-4):261 – 266, 1992.

[7] K. Pachucki and A. M. Moro. Nuclear polarizability of helium isotopes in atomic transitions. *Phys. Rev. A*, 75(3):032521, Mar 2007.

[8] J. L. Friar and G. L. Payne. Nuclear polarizabilities and logarithmic sum rules. *Phys. Rev. C*, 55(6):2764–2767, 1997.

[9] D. R. Phillips, G. Rupak, and M. J. Savage. Improving the convergence of nn effective field theory. *Phys. Lett.*, B473(3-4):209 – 218, 2000.

[10] I. Stetcu, S. Quaglioni, J. L. Friar, A. C. Hayes, and Petr Navrátil. Electric dipole polarizabilities of hydrogen and helium isotopes. *Phys. Rev. C*, 79(6): 064001, Jun 2009.

[11] Victor D. Efros, Winfried Leidemann, and Giuseppina Orlandini. Photodisintegration of the three-nucleon systems and their polarizabilities. *Phys. Lett.*, B408(1-4):1 – 6, 1997.

[12] R. Krivec, B. Golli, M. Rosina, and S. Sirca, editors. *Few-Body Problems in Physics '02*, volume 14. Springer-Verlag Wein, New York, 2003.

[13] M. Fischer et al. New limits on the drift of fundamental constants from laboratory measurements. *Phys. Rev. Lett.*, 92(23):230802, Jun 2004.

[14] Savely G. Karshenboim. Precision physics of simple atoms: Qed tests, nuclear structure and fundamental constants. *Phys. Rep.*, 422(1-2):1 – 63, 2005.

[15] Peter J. Mohr, Barry N. Taylor, and David B. Newell. Codata recommended values of the fundamental physical constants: 2006. *Rev. Mod. Phys.*, 80(2): 633–730, Jun 2008.

[16] Ingo Sick. On the rms-radius of the proton. *Physics Letters B*, 576(1-2):62 – 67, 2003.

[17] Y. M. Shin, D. M. Skopick, and J. J. Murphy. Properties of halo nuclei from atomic isotope shifts. *Can. J. Phys.*, 835:311, 2005.

[18] D. A. Varshalovich, A. N. Moskalev, and V. K. Khersonskii. *Quantum Thoery of Angular Momentum*. World Scientific, Singapore, 1988.

[19] S. Bacca. PhD thesis, Universities Mainz and Trento, 2005.

[20] Nir Barnea, Winfried Leidemann, and Giuseppina Orlandini. Ground state wave functions in the hyperspherical formalism for nuclei with a¿4. *Nuclear Physics A*, 650(4):427 – 442, 1999.

[21] Nir Barnea and Akiva Novoselsky. Construction of hyperspherical functions symmetrized with respect to the orthogonal and the symmetric groups. *Annals of Physics*, 256(2):192 – 225, 1997.

[22] Nir Barnea and Akiva Novoselsky. Hyperspherical wave functions with orthogonal and permutational symmetry. *Phys. Rev. A*, 57(1):48–58, Jan 1998.

[23] D. R. Thompson, M. Lemere, and Y. C. Tang. Systematic investigation of scattering problems with the resonating-group method. *Nuclear Physics A*, 286(1):53 – 66, 1977.

[24] I. Reichstein and Y.C. Tang. Study of n + [alpha] system with the resonating-group method. *Nuclear Physics A*, 158(2):529 – 545, 1970.

[25] R. B. Wiringa and Steven C. Pieper. Evolution of nuclear spectra with nuclear forces. *Phys. Rev. Lett.*, 89(18):182501, Oct 2002. doi:10.1103/PhysRevLett.89.182501.

[26] R. A. Malfliet and J. A. Tjon. Solution of the faddeev equations for the triton problem using local two-particle interactions. *Nuclear Physics A*, 127(1): 161 – 168, 1969.

[27] J. L. Friar. Nuclear polarization corrections in $\mu - he4$ atoms. *Phys. Rev. C*, 16(4):1540–1548, 1977.

Appendix A

Complete Derivations of Sum Rule Formulas

I have attempted to provide convincing derivations of all of the sum rules formulas that were cited in this work.

A.1 Thomas-Reiche-Kuhn Sum Rule

A.1.1

$$
\begin{aligned}
\Sigma^{TRK} &= \mathscr{G} \sum_n |\langle n| D_z |0\rangle|^2 (E_n - E_0), \\
&= \mathscr{G} \sum_n \langle 0| D_z |n\rangle \langle n| D_z |0\rangle (E_n - E_0), \\
&= \mathscr{G} \sum_n \langle 0| D_z |n\rangle (E_n - E_0) \langle n| D_z |0\rangle, \\
&= \mathscr{G} \sum_n \frac{1}{2} \langle 0| D_z |n\rangle (E_n - E_0) \langle n| D_z |0\rangle - \frac{1}{2} \langle 0| D_z |n\rangle (E_0 - E_n) \langle n| D_z |0\rangle, \\
&= \mathscr{G} \sum_n \frac{1}{2} \left(\langle 0| D_z |n\rangle \langle n| (E_n D_z - D_z E_0) |0\rangle - \langle 0| (E_0 D_z - D_z E_n) |n\rangle \langle n| D_z |0\rangle \right), \\
&= \mathscr{G} \sum_n \frac{1}{2} \left(\langle 0| D_z |n\rangle \langle n| (H D_z - D_z H) |0\rangle - \langle 0| (H D_z - D_z H) |n\rangle \langle n| D_z |0\rangle \right), \\
&= \mathscr{G} \sum_n \frac{1}{2} \left(\langle 0| D_z |n\rangle \langle n| [H, D_z] |0\rangle - \langle 0| [H, D_z] |n\rangle \langle n| D_z |0\rangle \right), \\
&= \frac{\mathscr{G}}{2} \left(\langle 0| D_z [H, D_z] |0\rangle - \langle 0| [H, D_z] D_z |0\rangle \right), \\
&= \frac{\mathscr{G}}{2} \langle 0| [D_z, [H, D_z]] |0\rangle .
\end{aligned}
$$

A.1.2

We can split the Haniltonian into a kinetic and potential energy part $H = T + V$:

$$
\frac{\mathscr{G}}{2} \langle 0| [D_z, [H, D_z]] |0\rangle = \frac{\mathscr{G}}{2} \left(\langle 0| [D_z, [T, D_z]] |0\rangle + \langle 0| [D_z, [V, D_z]] |0\rangle \right),
$$

where T is the kinetic energy and V is the potential.

We can further simplify the kinetic energy part by actually calculating the commutators. Two possible choices of coordinates in which the dipole is easy to define are the lab frame and the centre-of-mass frame.

Using lab-frame coordinaties

$$
\begin{aligned}
&\mathbf{P}_{CM} = \sum_{i=1}^{A} \mathbf{p}_i, \\
&\mathbf{R}_{CM} = \frac{1}{A} \sum_{i=1}^{A} \mathbf{r}_i, \\
&[\mathbf{P}_{CM}, \mathbf{R}_{CM}] = -i\hbar, \\
&[\mathbf{p}_i, \mathbf{R}_{CM}] = \frac{1}{A} \sum_{j=1}^{A} [\mathbf{p}_i, \mathbf{r}_j] = \frac{-i\hbar}{A}, \\
&[\mathbf{P}_{CM}, \mathbf{r}_i] = \sum_{j=1}^{A} \left[\mathbf{p}_j, \mathbf{r}_i\right] = -i\hbar, \\
&T_{\text{int}} = T_{\text{lab}} - T_{\text{CM}} = \frac{1}{2m} \left(\sum_{i=1}^{A} \mathbf{p}_i^2 - \frac{1}{A} \mathbf{P}_{CM}^2 \right), \\
&D_z = \sum_{i=1}^{A} (\mathbf{r}_i - \mathbf{R}_{CM}) \, q_i = \sum_{i=1}^{A} \mathbf{r}_i q_i - Z\mathbf{R}_{CM}.
\end{aligned}
$$

First calculate $[T, D_z]$.

$$
\begin{aligned}
[T, D_z] &= \frac{1}{2m} \left[\sum_{i=1}^{A} \mathbf{p}_i^2 - \frac{1}{A} \mathbf{P}_{CM}^2, \sum_{j=1}^{A} \mathbf{r}_j q_j - Z\mathbf{R}_{CM} \right], \\
&= \frac{1}{2m} \left(\sum_{i=1}^{A} \sum_{j=1}^{A} \left[\mathbf{p}_i^2, \mathbf{r}_j q_j\right] - \sum_{i=1}^{A} \left[\mathbf{p}_i^2, Z\mathbf{R}_{CM}\right] - \sum_{j=1}^{A} \left[\frac{1}{A} \mathbf{P}_{CM}^2, \mathbf{r}_j q_j \right] + \left[\frac{1}{A} \mathbf{P}_{CM}^2, Z\mathbf{R}_{CM} \right] \right), \\
&= \frac{1}{2m} \left(\sum_{i=1}^{A} \sum_{j=1}^{A} \left(\mathbf{p}_i \left[\mathbf{p}_i, \mathbf{r}_j\right] q_j + \left[\mathbf{p}_i, \mathbf{r}_j\right] \mathbf{p}_i q_j \right) - \sum_{i=1}^{A} 2Z \left[\mathbf{p}_i, \mathbf{R}_{CM}\right] \mathbf{p}_i - \sum_{j=1}^{A} \frac{2}{A} \left[\mathbf{P}_{CM}, \mathbf{r}_j\right] \mathbf{P}_{CM} + \frac{2Z}{A} \left[\mathbf{P}_{CM}, \mathbf{R}_{CM}\right] \mathbf{P}_C \right. \\
&= \frac{-i\hbar}{m} \left(\sum_{i=1}^{A} \mathbf{p}_i q_i - \sum_{i=1}^{A} \frac{Z}{A} \mathbf{p}_i - \sum_{j=1}^{A} \frac{1}{A} \mathbf{P}_{CM} q_j + \frac{Z}{A} \mathbf{P}_{CM} \right), \\
&= \frac{-i\hbar}{m} \left(\sum_{i=1}^{A} \left(q_i - \frac{Z}{A} \right) \mathbf{p}_i - \frac{Z}{A} \mathbf{P}_{CM} + \frac{Z}{A} \mathbf{P}_{CM} \right), \\
&= \frac{-i\hbar}{m} \sum_{i=1}^{A} \left(q_i - \frac{Z}{A} \right), \mathbf{p}_i
\end{aligned}
$$

Now calculate $[D_z,[T,D_z]]$.

$$\begin{aligned}
[D_z,[T,D]] &= \frac{-i\hbar}{m}\left[\sum_{i=1}^{A}\mathbf{r}_i q_i - Z\mathbf{R}_{CM}, \sum_{j=1}^{A}\left(q_j-\frac{Z}{A}\right)\mathbf{p}_j\right], \\
&= \frac{-i\hbar}{m}\left(\sum_{i=1}^{A}\sum_{j=1}^{A}\left[\mathbf{r}_i q_i, \left(q_j-\frac{Z}{A}\right)\mathbf{p}_j\right] - \sum_{j=1}^{A}\left[Z\mathbf{R}_{CM}, \left(q_j-\frac{Z}{A}\right)\mathbf{p}_j\right]\right), \\
&= \frac{-i\hbar}{m}\left(\sum_{i=1}^{A}\sum_{j=1}^{A} q_i\left(q_j-\frac{Z}{A}\right)\left[\mathbf{r}_i,\mathbf{p}_j\right] - \sum_{j=1}^{A} Z\left(q_j-\frac{Z}{A}\right)\left[\mathbf{R}_{CM},\mathbf{p}_j\right]\right), \\
&= \frac{\hbar^2}{m}\left(\sum_{i=1}^{A}\left(q_i^2 - q_i\frac{Z}{A}\right) - \sum_{j=1}^{A} Z\left(q_j-\frac{Z}{A}\right)\frac{1}{A}\right), \\
&= \frac{\hbar^2}{m}\left(Z - \frac{Z^2}{A} - \left(\frac{Z^2}{A}-\frac{Z^2}{A}\right)\right), \\
&= \frac{\hbar^2}{m}\left(\frac{Z(Z+N)}{A} - \frac{Z^2}{A}\right), \\
&= \frac{\hbar^2}{m}\frac{ZN}{A}.
\end{aligned}$$

Then we have:

$$\begin{aligned}
\Sigma^{TRK} &= \frac{\mathscr{G}}{2}\langle 0|\left[D_z,[H,D_z]\right]|0\rangle, \\
&= \frac{\mathscr{G}}{2}\frac{\hbar^2}{m}\frac{ZN}{A}\left(1+\kappa^{TRK}\right),
\end{aligned}$$

where

$$\kappa^{TRK} = \frac{mA}{\hbar^2 NZ}\langle 0|\left[D_z,[V,D_z]\right]|0\rangle.$$

Using centre-of-mass frame coordinates

First we have to derive the commutators. As before we have:

$$\begin{aligned}
\mathbf{P}_{CM} &= \sum_{i=1}^{A} \mathbf{p}_i, \\
\mathbf{R}_{CM} &= \frac{1}{A} \sum_{i=1}^{A} \mathbf{r}_i, \\
[\mathbf{p}_i, \mathbf{R}_{CM}] &= \frac{1}{A} \sum_{j=1}^{A} [\mathbf{p}_i, \mathbf{r}_j] = \frac{-i\hbar}{A}, \\
[\mathbf{P}_{CM}, \mathbf{r}_i] &= \sum_{j=1}^{A} \left[\mathbf{p}_j, \mathbf{r}_i\right] = -i\hbar, \\
[\mathbf{P}_{CM}, \mathbf{R}_{CM}] &= -i\hbar,
\end{aligned}$$

Now we define the centre-of-mass frame coordinates:

$$\begin{aligned}
\mathbf{r'}_i &= \mathbf{r}_i - \mathbf{R}_{CM}, \\
\mathbf{p'}_i &= \mathbf{p}_i - \mathbf{P}_{CM}.
\end{aligned}$$

Thus the commutators are:

$$\begin{aligned}
\left[\mathbf{p'}_i, \mathbf{r'}_j\right] &= \left[\mathbf{p}_i - \frac{1}{A}\mathbf{P}_{CM}, \mathbf{r}_j - \mathbf{R}_{CM}\right], \\
&= [\mathbf{p}_i, \mathbf{r}_j] - [\mathbf{p}_i, \mathbf{R}_{CM}] - \frac{1}{A}[\mathbf{P}_{CM}, \mathbf{r}_j]\frac{1}{A}[\mathbf{P}_{CM}, \mathbf{R}_{CM}], \\
&= \delta_{ij}(-i\hbar) - \frac{1}{A}(-i\hbar) - \frac{1}{A}(-i\hbar) + \frac{1}{A}(-i\hbar), \\
&= \left(\delta_{ij} - \frac{1}{A}\right)(-i\hbar), \\
\left[\mathbf{P}_{CM}, \mathbf{r'}_i\right] &= [\mathbf{P}_{CM}, \mathbf{r}_i - \mathbf{R}_{CM}] = (-i\hbar) - (-i\hbar) = 0, \\
\left[\mathbf{p'}_i, \mathbf{R}_{CM}\right] &= \left[\mathbf{p}_i - \frac{1}{A}\mathbf{P}_{CM}, \mathbf{R}_{CM}\right] = \frac{1}{A}(-i\hbar) - \frac{1}{A}(-i\hbar) = 0.
\end{aligned}$$

Now we observe that in these coordinates:

$$T_{\text{int}} = \frac{1}{2m}\sum_{i=1}^{A}\mathbf{p}'^{2}_{i},$$
$$D_z = \sum_{i=1}^{A} q_i \mathbf{r}'_i.$$

We precede thus:

$$\begin{aligned}
[T, D_z] &= \frac{1}{2m}\sum_{i=1}^{A}\sum_{j=1}^{A}\left[\mathbf{p}'^{2}_{i}, \mathbf{r}'_j q_j\right], \\
&= \frac{1}{2m}\sum_{i=1}^{A}\sum_{j=1}^{A}\left(\mathbf{p}'_i\left[\mathbf{p}'_i, \mathbf{r}'_j\right]q_j + \left[\mathbf{p}'_i, \mathbf{r}'_j\right]q_j\right)), \\
&= \frac{-i\hbar}{m}\sum_{i=1}^{A}\sum_{j=1}^{A}\left(\delta_{ij} - \frac{1}{A}\right)\mathbf{p}'_i q_j, \\
&= \frac{-\hbar}{m}\left(\sum_{i=1}^{A}\mathbf{p}'_i q_i - \sum_{i=1}^{A}\sum_{j=1}^{A}\frac{1}{A}\mathbf{p}'_i q_j\right), \\
&= \frac{-i\hbar}{m}\sum_{i=1}^{A}\left(q_i - \frac{Z}{A}\right)\mathbf{p}'_i.
\end{aligned}$$

Then we can calculate:

$$\begin{aligned}
[D_z,[T,D_z]] &= \frac{-i\hbar}{m}\sum_{i=1}^{A}\sum_{j=1}^{A}\left[q_i\mathbf{r}'_i,\left(q_j-\frac{Z}{A}\right)\mathbf{p}'_i\right], \\
&= \frac{-i\hbar}{m}\sum_{i=1}^{A}\sum_{j=1}^{A}q_i\left(q_j-\frac{Z}{A}\right)\left[\mathbf{r}'_i,\mathbf{p}'_i\right], \\
&= \frac{\hbar^2}{m}\sum_{i=1}^{A}\sum_{j=1}^{A}q_i\left(q_j-\frac{Z}{A}\right)\left(\delta_{ij}-\frac{1}{A}\right), \\
&= \frac{\hbar^2}{m}\left(\sum_{i=1}^{A}q_i^2-\frac{Z}{A}q_i-\sum_{i=1}^{A}\sum_{j=1}^{A}q_i\left(q_j-\frac{Z}{A}\right)\frac{1}{A}\right), \\
&= \frac{\hbar^2}{m}\left(Z-\frac{Z}{A}-\left(\frac{Z^2}{A}-\frac{Z^2}{A}\right)\right), \\
&= \frac{\hbar^2}{m}\left(\frac{Z(Z+N)}{A}-\frac{Z^2}{A}\right), \\
&= \frac{\hbar^2}{m}\frac{NZ}{A}.
\end{aligned}$$

And so, as before:

$$\begin{aligned}
\Sigma^{TRK} &= \frac{\mathscr{G}}{2}\langle 0|\left[D_z,[H,D_z]\right]|0\rangle, \\
&= \frac{\mathscr{G}}{2}\frac{\hbar^2}{m}\frac{ZN}{A}\left(1+\kappa^{TRK}\right),
\end{aligned}$$

where

$$\kappa^{TRK} = \frac{mA}{\hbar^2 NZ}\langle 0|\left[D_z,[V,D_z]\right]|0\rangle.$$

A.2 Bremstrahlung Sum Rule

A.2.1

$$\begin{aligned}
\Sigma^{BSR} &= \mathscr{G}\sum_n |\langle n|D_z|0\rangle|^2, \\
&= \mathscr{G}\sum_n \langle 0|D_z|n\rangle\langle n|D_z|0\rangle, \\
&= \mathscr{G}\langle 0|D_z\sum_n |n\rangle\langle n|D_z|0\rangle, \\
&= \mathscr{G}\langle 0|D_z^\dagger D_z|0\rangle.
\end{aligned}$$

A.2.2

We can re-write the dipole operator in terms of $\mathbf{R}_{PN}$, the distance between the proton and neutron centres of mass:

$$\begin{aligned}
D_z &= \frac{1}{2}\sum_{i=1}^{A}\tau_i^z\mathbf{r}'_i, \\
&= \frac{1}{2}\left(\frac{N+Z}{A}\right)\sum_{i=1}^{A}\tau_i^z\mathbf{r}'_i, \\
&= \frac{1}{2}\frac{NZ}{A}\left(\frac{1}{Z}+\frac{1}{N}\right)\sum_{i=1}^{A}\tau_i^z\mathbf{r}'_i, \\
&= \frac{NZ}{A}\left(\frac{1}{Z}\sum_{i=1}^{A}\frac{\tau_i^z\mathbf{r}'_i}{2}+\frac{1}{N}\sum_{i=1}^{A}\frac{\tau_i^z\mathbf{r}'_i}{2}\right), \\
&= \frac{NZ}{A}\left(\frac{1}{Z}\sum_{i=1}^{A}\frac{(1+\tau_i^z)}{2}\mathbf{r}'_i-\frac{1}{N}\sum_{i=1}^{A}\frac{(1-\tau_i^z)}{2}\mathbf{r}'_i\right), \\
&= \frac{NZ}{A}\left(\mathbf{R}_{PCM}-\mathbf{R}_{NCM}\right) = \frac{NZ}{A}\mathbf{R}_{PN}.
\end{aligned}$$

[1]

Now we can re-wrtie the BSR sum:

$$\begin{aligned}\Sigma^{BSR} &= \mathscr{G}\left\langle 0\right| D_z^\dagger D_z \left|0\right\rangle, \\ &= \mathscr{G}\left(\frac{NZ}{A}\right)^2 \left\langle \mathbf{R}_{PN}^2 \right\rangle.\end{aligned}$$

A.2.3

Considering that we can also write the dipole operator as a sum over only the proton coordinates: $D_z = \sum_{i=1}^{Z} \mathbf{r}'_i$, we can derive the following relation:

$$\begin{aligned}D_z^\dagger D_z &= \sum_{i,j=1}^{Z} \mathbf{r}'_i \cdot \mathbf{r}'_j, \\ &= \frac{1}{2}\left(\mathbf{r}'^2_i + \mathbf{r}'^2_j - \left(\mathbf{r}'_i - \mathbf{r}'_j\right)^2\right), \\ &= \frac{1}{2}(2Z)\sum_{i=1}^{Z} \mathbf{r}'^2_i - \frac{1}{2}\sum_{i,j=1}^{Z}\left(\mathbf{r}'_i - \mathbf{r}'_j\right)^2, \\ &= Z^2\left\langle \mathbf{r}_p^2 \right\rangle - \frac{Z(Z-1)}{2}\left\langle \mathbf{r}_{pp}^2 \right\rangle,\end{aligned}$$

where $\mathbf{r}_p^2$ and $\mathbf{r}_{pp}^2$ are the mean-square proton radius and the mean square proton-proton distance respectively, defined as:

$$\begin{aligned}\mathbf{r}_p^2 &= \frac{1}{Z}\sum_{i=1}^{Z} \mathbf{r}'^2_i, \\ \mathbf{r}_{pp}^2 &= \frac{1}{Z(Z-1)}\sum_{i,j=1}^{Z}\left(\mathbf{r}'_i - \mathbf{r}'_j\right)^2.\end{aligned}$$

Then the BSR sum rule becomes:

$$\Sigma^{BSR} = \mathscr{G}\left(Z^2\left\langle \mathbf{r}_p^2 \right\rangle - \frac{Z(Z-1)}{2}\left\langle \mathbf{r}_{pp}^2 \right\rangle\right).$$

[1] Recal that since $\mathbf{r}'_i$ are the centre of mass coordinates, their sum over all particles is zero. Thus we can add arbitrary constant terms into the sum over $\mathbf{r}'_i$'s

A.2.4

Observe that since we're in the centre of mass, we can also re-write the dipole operator as $D_z = -\sum_{i=1}^{A}(1-q_i)\,\mathbf{r}'_i = -\sum_{i=1}^{N}\mathbf{r}'_i$. But then we have that

$$D_z^\dagger D_z = \sum_{i,j=1}^{N} \mathbf{r}'_i \cdot \mathbf{r}'_j,$$

which has the same form as the previous derivation only now we are summing over neturons instead of protons. Thus we can immediatley derive:

$$\Sigma^{BSR} = \mathscr{G}\left(N^2\left\langle \mathbf{r}_n^2\right\rangle - \frac{N(N-1)}{2}\left\langle \mathbf{r}_{nn}^2\right\rangle\right),$$

where $\mathbf{r}_n^2$ and $\mathbf{r}_{nn}^2$ are defined similarly as for protons.

A.2.5

We can also consider the following form for $D_z^\dagger D_z$:

$$D_z^\dagger D_z = \sum_{i,j=1}^{A} \frac{\tau_i^z \tau_j^z \mathbf{r}'_i \cdot \mathbf{r}'_j}{4}.$$

We can split this sum into proton-proton, neutron-neutron, and proton-neutron pairs:

$$D_z^\dagger D_z = \frac{1}{4}\sum_{i,j=1}^{Z} \mathbf{r}'_i \cdot \mathbf{r}'_j + \frac{1}{4}\sum_{i,j=1}^{N} \mathbf{r}'_i \cdot \mathbf{r}'_j - \frac{1}{4}2\sum_{i=1}^{Z}\sum_{i=1}^{N} \mathbf{r}'_i \cdot \mathbf{r}'_j,$$

where we introduce a factor of 2 in the third term because the original sum would double-count each pair. We see that the first two terms, from previous analysis, are multiples of the dipole square-norm:

$$D_z^\dagger D_z = \frac{1}{4}D_z^\dagger D_z + \frac{1}{4}D_z^\dagger D_z - \frac{1}{4}2\sum_{i=1}^{Z}\sum_{i=1}^{N} \mathbf{r}'_i \cdot \mathbf{r}'_j.$$

Thus, we can regroup terms and proceed:

$$\begin{aligned} D_z^\dagger D_z &= -\sum_{i=1}^{Z}\sum_{i=1}^{N} \mathbf{r'}_i \cdot \mathbf{r'}_j \\ &= -\frac{1}{2}\left(\sum_{i=1}^{Z}\sum_{i=1}^{N} \mathbf{r'}_i^2 + \mathbf{r'}_j^2 - \sum_{i=1}^{Z}\sum_{i=1}^{N} \left(\mathbf{r'}_i - \mathbf{r'}_j\right)^2\right), \\ &= \frac{1}{2}\left(NZ\mathbf{r}_{pn}^2 - NZ\mathbf{r}_p^2 - NZ\mathbf{r}_n^2\right), \\ &= \frac{NZ}{2}\left(\mathbf{r}_{pn}^2 - \mathbf{r}_p^2 - \mathbf{r}_n^2\right), \end{aligned}$$

where $\mathbf{r}_{pn}^2$ is the mean-square proton-neutron distance:

$$\frac{1}{NZ}\sum_{i=1}^{Z}\sum_{i=1}^{N}\left(\mathbf{r'}_i - \mathbf{r'}_j\right)^2.$$

So then the BSR sum rule can be written:

$$\Sigma^{BSR} = \mathscr{G}\frac{NZ}{2}\left(\left\langle \mathbf{r}_{pn}^2 \right\rangle - \left\langle \mathbf{r}_p^2 \right\rangle - \left\langle \mathbf{r}_n^2 \right\rangle\right).$$

A.2.6

We can observe that the dipole magnitude is proportional to the magnitude of the proton centre of mass.

$$\begin{aligned} D_z^\dagger D_z &= \sum_{i,j=1}^{Z} \mathbf{r'}_i \cdot \mathbf{r'}_j, \\ &= Z^2\left(\frac{1}{Z^2}\sum_{i,j=1}^{Z} \mathbf{r'}_i \cdot \mathbf{r'}_j\right), \\ &= Z^2\mathbf{R}_p^2. \end{aligned}$$

Then we can see that:

$$\begin{aligned}
D_z^\dagger D_z &= \sum_{i,j=1}^{Z} \mathbf{r'}_i \cdot \mathbf{r'}_j, \\
&= 2\sum_{i=1}^{Z} \mathbf{r'}_i \sum_{i=1}^{Z} \mathbf{r'}_j - Z^2 \mathbf{R}_p, \\
&= 2Z\sum_{i=1}^{Z} \mathbf{r'}_i \mathbf{R}_p - Z\sum_{i=1}^{Z} \mathbf{R}_p^2, \\
&= -Z\sum_{i=1}^{Z} \left(\mathbf{r'}_i^2 - \mathbf{r'}_i^2 - 2\mathbf{r'}_i \mathbf{R}_p + \mathbf{R}_p^2 \right), \\
&= Z\sum_{i=1}^{Z} \left(\mathbf{r'}_i^2 - \left(\mathbf{r'}_i - \mathbf{R}_p \right)^2 \right), \\
&= Z^2 \mathbf{r}_p^2 - Z^2 \mathbf{r'}_p^2,
\end{aligned}$$

where $\mathbf{r'}_p^2$ is the mean square distrance between protons and the proton centre of mass:

$$\mathbf{r'}_p^2 = \frac{1}{Z}\sum_{i=1}^{Z} \left(\mathbf{r'}_i - \mathbf{R}_p \right)^2.$$

This gives us another expression for the BSR sum rule:

$$\Sigma^{BSR} = \mathscr{G}\left(Z^2 \left\langle \mathbf{r}_p^2 \right\rangle - Z^2 \left\langle \mathbf{r'}_p^2 \right\rangle \right).$$

A.3 Polarizability Sum Rule

A.3.1

$$
\begin{aligned}
\Sigma^{PSR} &= \int_{\omega_{th}}^{\infty} d\omega \mathscr{G} \frac{R(\omega)}{\omega}, \\
&= \int_{\omega_{th}}^{\infty} d\omega \frac{\mathscr{G}}{\omega} \sum_n |\langle n| D_z |0\rangle|^2 \, \delta(E_n - E_0 - \omega), \\
&= \mathscr{G} \sum_n \frac{\langle 0| D_z^\dagger |n\rangle \langle n| D_z |0\rangle}{E_n - E_0}, \\
&= \mathscr{G} \sum_n \frac{\langle 0| D_z^\dagger |n\rangle \langle n| D_z |0\rangle}{H - E_0}, \\
&= \mathscr{G} \langle 0| \frac{D_z^\dagger D_z}{H - E_0} |0\rangle, \\
&= -\mathscr{G} \langle 0| \frac{D_z^\dagger D_z}{E_0 - H} |0\rangle .
\end{aligned}
$$

Appendix B

Hyperspherical Formalism

Here I have presented some more details about the hyperspherical formalism. The main ideas are sketched, while the more technical derivations are left out.

B.1 Jacobi Coordinates

The hyperspherical coordinates are recursively defined in terms of a set of Jacobi coordinates. Jacobi coordinates are an extension of the technique used in the two-body problem with a central potential where the center of mass motion is ignored and the relative position vector between the two masses is imagined as the position vector of a single pseudo-particle.

The Jacobi coordinates for a two body system are the magnitude and two angles associated with the vector from the regular two-body problem. In a four-body system, we first pick two particles and their relative position vector as before. Next we take the position vector of the third particle with respect to the centre of mass of the first two, and then the relative position of the fourth particle with respect to the centre of mass of the first three. This is illustrated in Figure B.1

We continue this process up to A particles, thus defining $A-1$ lengths and $2(A-1)$ angles. These are the Jacobi coordinates of the system. It's easy to see that for A identical mass particles with positions $\mathbf{r}_k$ in the lab frame, the k^{th} Jacobi

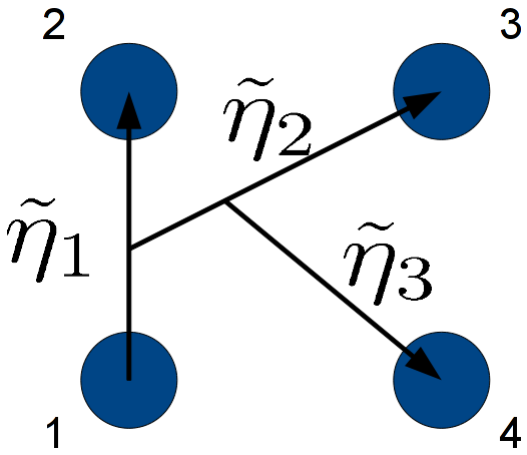

Figure B.1: The (unnormalized) Jacobi coordinates for four particles. The $\tilde{\eta}_i$ vectors point along the direction of the normalized η_i given by equation (B.1).

coordinate is defined:

$$\eta_k = \sqrt{\frac{k}{k+1}}\left(\mathbf{r}_{k+1} - \frac{1}{k}\sum_{i=1}^{k}\mathbf{r}_i\right) \qquad k = 1,...,A-1. \tag{B.1}$$

B.2 Hyperspherical Coordinates and the Laplace Operator

Suppose we have a set of $A-1$ Jacobi coordinates $\{\eta_k\}$ with magnitudes η_k and angular parts $\hat{\eta}_k$. Then we define the first hyper-radial coordinate $\rho_1 = \eta_1$ and the k^{th} hyper-radial coordinate is defined such that:

$${\rho_k}^2 = \sum_{i=1}^{k}{\eta_i}^2 = \frac{1}{k}\sum_{i<j}^{k+1}(\mathbf{r}_i - \mathbf{r}_j)^2. \tag{B.2}$$

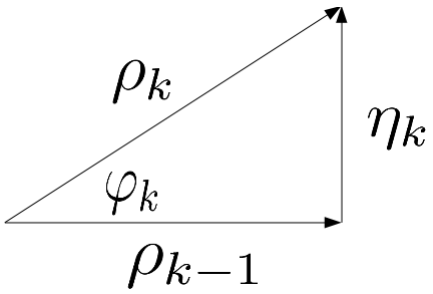

Figure B.2: Geometric interpretation of the recursive generation of hyperspherical coordinates

The the k^{th} hyperangle is defined such that:

$$\rho_{k-1} = \rho_k \cos(\varphi_k),$$
$$\eta_k = \rho_k \sin(\varphi_k).$$

We can visualize this geometrically (as shown in Figure B.2) by placing the previous hyper-radius and the next Jacobi coordinate on a plane at right angles. Then the magnitude of their difference is the next hyper radius, and the angle between the hyper-radii is the next hyper-angle.

One can show that, if $d\hat{\eta}_1$ and $d\hat{\eta}_2$ are the volume elements of the angular parts of the first two Jacobi coordinates in a three-body problem, then the total volume element in the hyperspherical coordinates for the three-body problem is

$$dV_6 = {\rho_2}^5 d\rho_2 \sin^2(\varphi_2) cos^2(\varphi_2) d\varphi_2 d\hat{\eta}_1 d\hat{\eta}_2 \equiv {\rho_2}^5 d\rho_2 dS_5,$$

and then the A body volume element can be defined recursively:

$$dV_{3(A-1)} = {\rho_{A-1}}^{3A-4} d\rho_{A-1} dS_{3A-4} \equiv {\rho_{A-1}}^{3A-4} d\rho_{A-1} \sin^2(\varphi_{A-1}) \cos^{3A-7}(\varphi_{A-1}) d\varphi_{A-1} d\hat{\eta}_{A-1} dS_{3A-7}.$$

Note that the volume element only depends on the last hyper-radial coordinate and all the angles, but not on any lower-order radial coordinates. As we will see, this is a useful property for evaluating matrix elements in hyperspherical coordinates.

As we can see from (B.2), the hyper-radial coordinate does not depend on which Jacobi coordinates are used and is symmetric under the permutation of particle positions. The whole A body system can thus be described by the centre of mass motion plus one hyper-radial coordinate ρ_A, $A-2$ hyper-angular coordinates $\varphi_{(A-1)} = \{\varphi_2, ...\varphi_{A-1}\}$, and $2(A-1)$ angular coordinates $\Omega_{(A-1)} = \{\hat{\eta}_1, ..., \hat{\eta}_{A-1}\}$. (Note that the angular and hyper-angular coordinates *do* depend on the choice of Jaboci coordinates).

Since it appears in the Schödinger equation, we must derive the Laplace operator in hyperspherical coordinates. Recall that for a two-body system, we can write the Laplace operator as

$$\Delta_{(1)} = \Delta_{\eta_1} - \frac{1}{{\eta_1}^2}\widehat{l_1^2},$$

where

$$\Delta_{\eta_1} = \frac{\partial^2}{\partial {\eta_1}^2} + \frac{2}{\eta_1}\frac{\partial}{\partial \eta_1},$$

and $\widehat{l_1}$ is the relative angular momentum operator. We can easily see that for the three-body problem expressed with two Jacobi coordinates, the Laplace operator becomes

$$\Delta_{(2)} = \Delta_{\eta_1} + \Delta_{\eta_2} - \frac{1}{{\eta_1}^2}\widehat{l_1^2} - \frac{1}{{\eta_2}^2}\widehat{l_2^2}.$$

If we apply the transformation into hyperspherical coordinates directly, we find that we can split the Laplace operator into a term that depends only on the hyper-radial coordinate, and an angular term:

$$\Delta_{(2)} = \Delta_{\rho_2} - \frac{1}{{\rho_2}^2}\widehat{K_2^2},$$

where

$$\Delta_{\rho_2} = \frac{\partial^2}{\partial {\rho_2}^2} + \frac{5}{\rho_2}\frac{\partial}{\partial \rho_2},$$

and

$$\widehat{K_2^2} = -\frac{\partial^2}{\partial {\varphi_2}^2} - 4\cot(2\varphi)\frac{\partial}{\partial \varphi_2} + \frac{1}{\cos^2(\varphi_2)}\widehat{l_1^2} + \frac{1}{\sin^2(\varphi_2)}\widehat{l_2^2}.$$

We want to recursively define $\Delta_{\rho_{A-1}}$ and $\frac{1}{{\rho_{A-1}}^2}\widehat{K_{A-1}^2}$ to be the radial and angular part

of $\Delta_{(A-1)}$. To do this we first observe that

$$\Delta_{(A-1)} \equiv \Delta_{\rho_{A-1}} - \frac{1}{{\rho_{A-1}}^2}\widehat{K}^2_{A-1}, \tag{B.3}$$

$$= \Delta_{\rho_{A-2}} - \frac{1}{{\rho_{A-2}}^2}\widehat{K}^2_{A-2} + \Delta_{\eta_{A-1}} - \frac{1}{{\eta_{A-1}}^2}\widehat{l}^2_{A-1}. \tag{B.4}$$

Then we transform ρ_{A-2} and η_{A-1} into ρ_{A-1} and φ_{A-1}. Equating (B.3) and (B.4) gives:

$$\Delta_{\rho_{A-1}} = \frac{\partial^2}{\partial {\rho_{A-1}}^2} + \frac{3(A-1)-1}{\rho_{A-1}}\frac{\partial}{\partial \rho_{A-1}},$$

and

$$\widehat{K}^2_{A-1} = -\frac{\partial^2}{\partial {\varphi_{A-1}}^2} + \frac{3A-9-(3A-5)\cos(2\varphi_{A-1})}{\sin(2\varphi_{A-1})}\frac{\partial}{\partial \varphi_{A-1}} + \frac{\widehat{l}^2_{A-1}}{\sin^2\varphi_{A-1}} + \frac{\widehat{K}^2_{A-2}}{\cos^2\varphi_{A-1}}.$$

Defining $\widehat{L}_{A-1} = \widehat{L}_{A-2} + \widehat{l}_{A-1}$ as the total internal angular momentum of the A-body system, one can show that the operators

$$\widehat{\mathscr{K}_{A-1}} = \{\widehat{K}^2_{A-1}, ..., \widehat{K}^2_2, \widehat{L}^2_{A-1}, ..., \widehat{L}^2_2, \widehat{l}^2_{A-1}, ..., \widehat{l}^2_1, \widehat{L}^z_{A-1}\}$$

all commute with each other and thus a hyperspherical state can be described by the associated eigenvalues.

B.3 Hyperspherical Harmonics

One can see that the hyperpherical harmonics are an extension of the spherical harmonics in a multidimensional space. In 3-dimensional space, we consider the eigenfunctions of the $\widehat{l}$ operator, known as the spherical harmoics. We can ask what the $3(A-1)$ dimensional analogue of the spherical harmonics are, namely, the hyperspherical harmonics. We note that $\widehat{\mathscr{K}_1} = \{\widehat{l}^2_1, \widehat{l}^z\}$. Thus, by definition, the eigenfunctions of $\widehat{\mathscr{K}_1}$ are the spherical harmonics. We then ask that the hyperspherical harmonics of order $A-1$ be the eigenfunctions of $\widehat{\mathscr{K}_{A-1}}$.

We can construct such eigenfunctions recursively using the spherical harmonics. First consider the base case: $\widehat{\mathscr{K}_2} = \{\widehat{K}^2_2, \widehat{L}^2_2, \widehat{L}^z_2, \widehat{l}^2_1, \widehat{l}^2_2\}$. We can construct an eigenfunction of $\{\widehat{L}^2_2, \widehat{L}^z_2, \widehat{l}^2_1, \widehat{l}^2_2\}$ by standard angular momentum coupling (for any

operator $\hat{Q}$, Q refers to the corresponding quantum number):

$$\Phi_{L_2M_2;l_1l_2}\left(\Omega_{(2)}\right) = \sum_{m1,m2} C^{L_2M_2}_{l_1m_1l_2m_2} Y_{l_1m_1}(\hat{\eta}_1) Y_{l_2m_2}(\hat{\eta}_2)$$

Where Y_{lm} refers to the spherical harmonic with angular momentum l and projection z and $C^{L_2M_2}_{l_1m_1l_2m_2}$ are the Clebsch-Gordan Coefficients [18].

The eigenfunctions of $\widehat{K}_2^2$ (with eigenvalues $K_2(K_2+4)$, $K_2 \geq l_1+l_2$) are given by [20]:

$$\psi_{K_2;l_1l_2}(\varphi_2) = \mathscr{N}(K_2,l_1,l_2)\left(\cos(\varphi_2)\right)^{l_1}\left(\sin(\varphi_2)\right)^{l_2} P_{n_2}^{(l_2+\frac{1}{2},l_1+\frac{1}{2})}\cos(2\varphi_2),$$

where $P_{n_2}^{(l_2+\frac{1}{2},l_1+\frac{1}{2})}$ is a Jacobi polynomial, $n_2 = \frac{K_2-l_1-l_2}{2}$, and

$$\mathscr{N}_2(K_2,l_1,l_2) = \sqrt{\frac{(2K_2+4)n_2!\Gamma(n_2+l_1+l_2+2)}{\Gamma(n_2+l_2+\frac{3}{2})\Gamma(n_2+l_1+\frac{3}{2})}}.$$

Then, since $\widehat{\mathscr{K}_2}$ all commute, we construct the hyperspherical harmonic

$$\mathscr{Y}_{\mathscr{K}_2}(\Omega_{(2)},\varphi_{(2)}) = \psi_{K_2;l_1l_2}(\varphi_2)\,\Phi_{L_2M_2;l_1l_2}\left(\Omega_{(2)}\right),$$

where $\mathscr{K}_{A-1}$ are the set $\{K_{A-1},...,K_2,L_{A-1},...,L_2,l_{A-1},...,l_1,M_{A-1}\}$ of quantum numbers associtated with $\widehat{\mathscr{K}_{A-1}}$.

We recall that since $\mathscr{K}_1 = \{l_1,m_1\}$, $\mathscr{Y}_{\mathscr{K}_1} = Y_{l_1m_1}$. We can now define a recursive procedure to construct higher order hyperspherical harmonics. Given $\mathscr{Y}_{\mathscr{K}_{A-2}}$ we construct $\mathscr{Y}_{\mathscr{K}_{A-1}}$ by first coupling $Y_{l_{A-1}m_{A-1}}$ to $\mathscr{Y}_{\mathscr{K}_{A-2}}$:

$$\Phi_{L_{A_1}M_{A-1};\mathscr{K}_{A-2}l_{A-1}}\left(\Omega_{(A-1)}\right) = \sum_{M_{A-2},m_{A-1}} C^{L_{A-1}M_{A-1}}_{l_{A_2}m_{A-2}l_{A-1}m_{A-1}} \mathscr{Y}_{\mathscr{K}_{A-2}}(\Omega_{(A-2)},\varphi_{A-2}) Y_{l_{A-1}m_{A-1}}(\hat{\eta}_{A-1}).$$

Then we construct the eigenfunction of $\widehat{K}_{A-1}^2$ with eigenvalue $K_{A-1}(K_{A-1}+3A-5)$ [20]

$$\psi_{K_{A-1};l_1K_{A-1}}(\varphi_{A-1}) = \mathscr{N}(K_{A-1},l_1,K_{A-2})\left(\cos(\varphi_{A-1})\right)^{K_{A-2}}\left(\sin(\varphi_{A-1})\right)^{l_{A-1}} P_{n_{A-1}}^{(l_{A-1}+\frac{1}{2},K_{A-2}+\frac{1}{2})}\cos(2\varphi_{A-1}),$$

where $n_{A-1} = \frac{K_{A-1}-K_{A-2}-l_{A-1}}{2}$ and

$$\mathscr{N}_{A-1}(K_{A-1}, l_1, K_{A-2}) = \sqrt{\frac{(2K_{A-1}+3A-5)n_{A-1}!\Gamma(n_{A-1}+K_{A-2}+l_{A-1}+\frac{3A-5}{2})}{\Gamma(n_{A-1}+l_{A-1}+\frac{3}{2})\Gamma(n_{A-1}+K_{A-2}+\frac{3A-6}{2})}}.$$

And finally, since all of $\widehat{\mathscr{K}_{A-1}}$ commute, we can construct the $(A-1)^{th}$ order hyperspherical harmonic

$$\mathscr{Y}_{\mathscr{K}_{A-1}}\left(\Omega_{(A-1)}, \varphi_{(A-1)}\right) = \psi_{K_{A-1};l_{A-1}K_{A-2}}\left(\varphi_{(A-1)}\right)\Phi_{L_{A-1}M_{A-1}};\mathscr{K}_{A-2}l_{A-1}\left(\Omega_{(A-1)}, \varphi_{(A-2)}\right). \tag{B.5}$$

Thus defined, the hyperspherical harmonics form an orthonaromal set of eigenfunctions on the hypersphere satisfying

$$\left\langle \mathscr{Y}_{\mathscr{K}_N} | \mathscr{Y}_{\mathscr{K}'_N} \right\rangle = \delta_{\mathscr{K}_N, \mathscr{K}'_N}.$$

B.4 Hyperspherical Basis

The hyperspherical harmonics as constructed above have no particular symmetry under particle permutation. One must construct completely antisymmetrized hyperspherical harmonics when dealing with fermions. The more difficult problem of generating anti-symmetrized hyperspherical harmonics is solved in [21, 22].

With anti-symmetrized harmonics, we can build the basis:

$$|K\rangle\,|\nu\rangle \equiv R_\nu(\rho)H_K(\Omega, s_1, \cdots, s_A, t_1, \cdots, t_A), labelbasis \tag{B.6}$$

where H_K is a hyperspherical harmonic and spin-isospin state which is totally antisymmetrized, K is a set of quantum numbers including a grandangular momentum, total angular momentum L with projection M, total spin/isospin S/T with projection S_z/T_z, as well as those related to permuational symmetry [20]. The hyper-radial part of the wave function (depending on ρ) needs to be expanded in a hyper-radial basis:

$$\psi(\rho) = \sum_\nu R_\nu(\rho).$$

The hyper-radial coordinate is a measure of the size of the system and we expect

the ground state wavefunction to fall off exponentially with hyper-radius, so we wish to use an expansion of the form

$$R_{K\nu}(\rho) = e^{-a\rho} P_\nu(\rho),$$

where $P_\nu(\rho)$ is a polynomial. A natural choice turns out to be the Laguerre Polynomials, because they satisfy the orthogonality relation

$$\int_0^\infty \rho^\alpha e^{-\rho} L_n^{(\alpha)}(\rho) L_m^{(\alpha)}(\rho) d\rho = \frac{(n+\alpha)!}{n!} \delta_{n,m},$$

and can be defined

$$L_n^{(\alpha)}(\rho) = \sum_{i=0}^{n} (-1)^i \binom{n+\alpha}{n-i} \frac{\rho^i}{i!}.$$

Then, the wavefunction is expanded

$$\Psi = \sum_{K\nu} C^{K\nu} R_\nu(\rho) H_K(\Omega, \sigma_1, \cdots, \sigma_A, \tau_1, \cdots, \tau_A) = \sum_{K\nu} C^{K\nu} |\nu\rangle |K\rangle .$$